Research Paper

Axial Load Capacity Predictions of Drilled Displacement Piles With SPT- and CPT-based Direct Methods

Genesis Figueroa[1], Antonio Marinucci[2], and Anne Lemnitzer[3]*

Abstract: Drilled Displacement Piles (DDP) provide an ideal foundation solution that combines the benefits of ground improvement with traditional advantages of piling systems. This paper offers insights gathered from 55 construction projects in which nearly 130 DDPs were installed and tested axially. High quality site exploration data (e.g., Cone Penetration Test (CPT) and Standard Penetration Test (SPT)) were evaluated to derive geotechnical analysis parameters. The test sites consisted of mostly mixed soil types with strongly stratified layers of sand, silt, and clay. Pile diameters ranged between 35 and 61 cm (14 to 24 inches). Prior to analyzing the axial performance of DDPs, a variety of failure interpretation methods were assessed to confidently extrapolate failure loads when field testing was terminated prior to pile failure. Results of this study suggested the Van der Veen's (1953) method to most closely estimate the load that triggers pile plunging behavior specific to DDPs, followed by the Butler & Hoy (1977) and L1-L2 methods (Hirany and Kulhawy, 1989). Hereafter, in-situ axial load test results were compared with a wide range of analytical methods, including those developed specifically for DDPs. Predictive accuracy was assessed in terms of total pile capacity and pile settlement and separated based on pile diameter, stiffness, and soil type. Most examined analytical methods underpredict the in-situ pile capacities for both, CPT and SPT -based analysis. It was also found that the difference between the experimentally determined and predicted capacities is related to the level of improvement in the surrounding soil following pile installation. A general comparison between predictive axial accuracy and the observed level of ground improvement is also discussed for sandy and mixed type of soils.

Keywords: pile analyses, drilled displacement piles, axial load tests, interpreted failure load, direct CPT methods, direct SPT methods, bearing capacity

Introduction

The use of Drilled Displacement Piles (DDP) is gaining increasing traction amongst the deep foundation industry. DDPs provide a fast and easy option to mitigate problematic in-situ conditions such as low bearing capacity, high settlements, and moderate liquefaction susceptibility. Particularly for sandy soils, DDP installation increases local soil resistance due to lateral displacement and compaction of adjacent soils (Siegel *et al.*, 2007). DDPs are advocated as ideal construction technique for projects near vibration-sensitive sites and in zones with contaminated soils given the lack of spoils during construction (i.e., environmentally friendly construction). Additionally, financial and time efficiency have been identified as key advantages to DDP installation when placed in suitable soil types (Basu and Prezzi, 2009).

The lateral soil displacement during pile installation strongly depends on the drilling tool, piling rig technology, and the installation parameters such as auger rotation, penetration rate, and installation torque during pile construction. Constructing DDPs involves a drilling process achieved with an axial force applied by a hydraulic machinery, and a simultaneous torque produced by the rotation of the drilling tool. Subsequently, concrete grout is either placed with a tremie, or injected under pressure, followed by the rebar cage placement. Most common DDP diameters range from 35 cm to 61 cm (14 to 24 inches) with lengths up to 30m (~100 ft); however, the use of larger diameters and longer lengths have increased, allowing auger displacement piles to be considered in a broader range of project sites.

Unlike driven piles, which can be inspected and monitored before and during pile driving, DDPs are known for their blind nature. Constructed DDPs require post installa-

[1] Graduate Student Researcher, Dept of Civil and Environmental Engineering, University of California Irvine, 4135 Engineering Gateway, Irvine, CA, 92697, USA
[2] President, V2C Strategists, LLC, 1177 Avenue of the Americas, 5th Floor, New York, NY 10036, USA
[3] Associate Professor, Dept of Civil and Environmental Engineering, University of California Irvine, 4135 Engineering Gateway, Irvine, CA, 92697, USA
* Corresponding author, email: alemnitz@uci.edu

Print ISSN: 1937-5247 Online ISSN: 1937-5255
Published by Deep Foundations Institute
Received 12 May 2022; received in revised form 12 August 2022; accepted 17 September 2022
https://doi.org/10.37308/DFIJnl.20220512.262

tion non-destructive testing to verify concrete quality and to detect potential areas where soil inclusions might have occurred. Alternatively, axial, and lateral load tests can be conducted to evaluate the global pile performance, including load capacity, tolerable settlements, and tolerable lateral displacements. Static pile load testing commonly consists of applying sequentially increasing axial loads, (typically in 5% increments of the design load) and measuring the axial displacement at the top of the pile. This procedure provides load-settlement curves from which the failure load can be obtained experimentally or theoretically depending on whether the maximum load was reached during the test. Based on the Caltrans – Foundation Manual: Ch. 8 "Static Pile Load Testing and Pile Dynamic Analysis", the static pile load testing on concrete piles is not recommended until the concrete reaches a minimum compressive strength of 13.8MPa (2000 psi).

To validate the design capacity, piles are commonly loaded to (1) their design loads plus a safety factor or (2) a large enough load to reach geotechnical failure. A popular approach is to load pile specimens to at least 200% of their calculated design load to assure sufficient axial capacity. The Federal Highway Administration's (FHWA) report on 'Static Testing of Deep Foundations' (FHWA-SA-91-042, 1992) highly recommends testing piles to failure whenever feasible, to "obtain the real safety factors intrinsic to the design". ASTM D1143M-20 (ASTM, 2020) also recommends reaching the failure load whenever possible to generate a rapid displacement of the foundation element so that further loading is not possible and plunging behavior is clearly visible in the load-settlement curve. As part of this study, the authors collected axial load test data from 55 different construction sites, in which 129 Drilled Displacement piles were tested axially. Within this newly established database, 33% of all piles were tested up to 2-2.5 times of their design load, 25% were tested up to 2.5-3 times of their design load, and 22% of piles were subjected to higher than 3 times their design load. The remaining 20% of all piles were subjected to an in-situ load less than two times the design load.

Current practice for the axial design of deep foundations employs different empirical methods developed between 1975 and today. Many of these methods have been validated and calibrated to approximate the failure load of driven and bored piles; only a few methods account for the installation and performance effects of specialty foundations such as drilled displacement piles (DDPs), Helical Piles, or Press-in Piles, unless specifically developed for such. The change of radial stresses during pile construction strongly depends on the pile installation technique and therefore directly impacts the pile-soil resistance and global pile performance. Nevertheless, axial methods are extrapolated and applied beyond their original development, either due to lack of an available method, due to highly unique field conditions, and/or for comparison.

This paper is the first of two papers in which the performance behavior of Drilled Displacement Piles is analyzed. The authors collected data from 55 construction sites, at which a total of 129 DDPs were tested either axially and/or laterally. The objective of this paper is to evaluate the axial performance behavior of Drilled Displacement piles and to provide valuable insight into the accuracy of existing SPT and CPT-based predictive methods in estimating the in- situ failure load of DDPs. Following a literature review on previous DDP research, the authors first assess a variety of literature-based methods used to interpret/estimate pile failure in the absence of experimentally reached failure, followed by a comparative statistical analysis of predicted and measured axial pile failure loads for DDPs in sand like, clay like, and mixed soil sites. The second paper in this series will assess the effects of the DDP installation on the surrounding soil using pre-and post CPT testing, and potential implications on the axial and lateral pile capacities. This study was conducted and supported as part of a DFI Technical Committee project, and data analyzed in both papers were provided by committee members with expertise in the construction and design of Drilled Displacement Piles.

Literature Review

Previous research on DDPs related to this study

Drilled displacement piles combine the effects of driven piles (axial force applied to the drilling tool) and torque applied by a continuous flight auger into the soil without soil removal. Consequently, soil-pile stress conditions are complex and highly dependent on the drilling tool. The insertion and rotation of the drilling tool produces not only shear, but cyclic lateral forces due to the rotation of the tool. Accordingly, the axial capacity of displacement piles is difficult to generalize.

Basu and Prezzi (2009) modeled the pile installation and axial loading via one-dimensional fine element analysis. The authors proposed an analytical method to estimate shaft resistance of DDPs installed in sandy soils by considering the effects of the drilling tool on the soil's relative density and level of confinement. Basu and Prezzi proposed the inclusion of a lateral earth pressure coefficient into the analysis of shaft resistance at limit state for different installation velocity ratios. The "before - after" ratio of the lateral earth pressure coefficient following pile installation, was found to be 2.2 to 2.7 times larger than the respective ratio for drilled shafts, and only 0.4 – 0.47 the ratio of traditional displacement piles. Similarly, the finite element analysis suggested the limit unit shaft resistance for DDPs to be larger than for drilled shaft (non-displacement piles) but lower than for jacked piles (displacement piles). The influence of the velocity of penetration and rotation ratio, and the effects on the radial stress surrounding the pile were also assessed in every construction phase (i.e., during the penetration and extraction of the drilling tool and the pile loading). Basu and Prezzi found the radial displacement of the soil during pile installation to reduce the radial stress around the pile shaft. Also, after the removal of the drilling tool, the torsional shear stress at the vicinity of the pile shaft becomes zero and the vertical shear stress reaches a negative limiting value. The installation effects, and therefore the relationship between the final and initial lateral earth pressure coefficient was proven to have a great impact on the shaft capacity of DDPs.

Stacho and Ladiscova (2014) numerically evaluated the soil improvement surrounding DDPs by considering the Cavity Expansion Theory (CET) by Mecsi (2013). Axial load-settlement curves were compared with results of two static load test and analytical predictions. The piles were located in a 10 m layer of soft clay followed by dense sand. Pile lengths ranged between 16 to 18 m and their diameter was 410 mm. FEM analyses which didn't model the soil improvement showed an underestimation of the real (in-situ) axial pile capacity of the DDP of up to 10%. To consider the soil improvement, tiny clusters with improved soil properties (based on CET results) were created around the pile vicinity to model the soil compaction. The modified FEM model showed a 98% accuracy between the model and the test data.

Shah and Deng (2016) studied the installation effects on the axial load response of four different piles installed in the same soil: drilled cast-in-place, continuous flight auger, drilled displacement, and drilled displacement steel piles. All piles had an identical length (12 m) and nearly identical diameters. The piles were heavily instrumented and axially tested to failure. The shaft resistance along the pile length and the toe resistance were recorded. At shallow depths, all piles indicated lower shaft resistance than analytically predicted. This (rather expected result) can be attributed to the low confinement stress at shallow depths and limited soil densification near the ground surface. For deeper layers, the shaft and tip resistance measured for the piles was higher than what the analytical methods suggested. The total axial capacity of the DDP was found to be 1.5 times higher than the capacity of the drilled shaft.

Moshfeghi and Eslami (2018) studied the reliability of CPT based predictions for axially loaded DDPs by specifically focusing on the installation technique and drilling tool. The results of 65 static load tests on DDPs were used to find a correlation between the predictive performance and drilling tool employed during pile construction. Moshfeghi and Eslami found the accuracy of the predicted pile capacity to be dependent on the drilling tool; for instance, the capacity of Atlas piles, a DDP type originating from Europe, was best predicted by the Brettmann and NeSmith (2005) method. The study also showed that for some CPT direct methods, the axial load capacity results are highly conservative for clayey soils.

Rad *et al*. (2021) studied the torque applied during construction, and the axial load performance of three different piles. A drilled displacement pile (DeWaal), a helical pile, and a Tsubasa pile (frequently used drilled displacement piles in Japan) were constructed and tested under compressive load. Two sets of experiments (large scale and model scale) were performed in the field and in the laboratory respectively; employing similar soil conditions: poorly graded sand (SP) with a friction angle between 32 - 34 degrees. The authors found that the DDP required a much higher torque compared to the other two piles, which was mainly attributed to the difference between the DDP diameter and the shaft diameter and geometry of the helical and Tsubasa pile. For all piles, the amount of torque needed to penetrate the soil was found to be proportional with depth. Even though the need of a lower torque during construction of the helical and Tsubasa piles might be seen as an advantage, the axial load test results suggested the performance of the DDP to be superior compared to the other two pile types. During the compression load test, the DDP reached a higher ultimate load, around 1.4 times higher than the helical and Tsubasa pile, and a lower settlement (~10%D) at failure.

Siegel *et al*. (2019) studied the end resistance of continuous flight auger (CFA) piles and drilled displacement piles in clayey soil with interbedded sand seams. Experimental data from 15 compression load tests were compared with analytical predictions of pile tip resistance Q_{tip} (i.e., $Q_{tip} = 9 \times Cu$, where Cu is the clay's undrained shear strength). A higher tip resistance was measured for both pile types in comparison with the conventional analytical estimate of 9 times the shear strength for bored piles. The authors did not find significant differences between the tip resistance of the CFA and the DDP piles, the latter was attributed to the type of soil in which both piles were installed and their amenability to improve the soil resistance due to the construction technique of the pile.

This study will complement the above-mentioned research efforts by evaluating the in-situ performance of Drilled Displacement piles in a variety of soil types. While much knowledge regarding the specific pile and soil performance exists within contractors and manufacturers of drilled displacement tooling, findings are not easily publishable due to data restrictions or non- disclosure agreements. With the generous provision of data by members of the DFI technical committees, the authors were able to collect the largest DDP database yet published and perform analysis of unprecedented comprehensiveness to help improve the design and analysis of this specialty piling technique.

Review of analytical and empirical methods to predict axial pile capacity

Depending on the availability and quality of the in-situ geotechnical data, two primary approaches to predict pile axial load capacity have emerged in geotechnical practice: indirect methods and direct methods. As implied by the name, direct methods use in-situ soil test data "directly" within their formulation, such as the blow count (N-SPT) of the standard penetration test (SPT), and the tip and side resistance (q_c and f_s, respectively) of the cone penetration test (CPT). In turn, indirect methods use geotechnical parameters estimated from empirical relationships, such as undrained shear strength (S_u), friction angle (ϕ), or the over-consolidation ratio (OCR). Due to the nature of this study and the objective to evaluate DDP using in-situ performance parameters, this paper will focus on the use of direct methods only, and hence indirect methods are excluded.

According to Eslami and Fellenius (1995), general North American geotechnical practice mostly employs the following methods for predicting axial pile capacities: Schmertmann and Nottingham (1975; 1978); DeRuiter and Beringen (1979); Bustamante and Gianeselli (1982),

also known as LCPC (Laboratoire Central des Ponts et Chaussées); Bustamante and Gianeselli (1993); and the Eurocode (1993). In addition to the aforementioned methods, this study also includes methods developed by Niazi and Mayne (2016) and Brettmann and NeSmith (2000-2005). Table 1 provides a summary of direct methods, including a detailed description for which types of piles these methods have been originally developed, and what geotechnical parameters (or measurements) are needed to calculate the pile's side friction and toe bearing resistance. Amongst all methods listed in Table 1, only Bustamante and Gianeselli (1993; 1998) as well as Brettmann and NeSmith (2000; 2005) were developed specifically for DDPs. Both methods were calibrated based on axial load test results, in-situ soil tests, and geo-mechanical soil properties obtained from empirical relations. Little information was provided on the effects of soil disturbance and the axial load capacity of the piles. Therefore, these two DDP methods are similarly narrowed to particular soil types, drilled displacement tools, and pile geometries as many of the above listed approaches. This limitation is common when empirical methodologies are developed based on proprietary information and/or technologies, predominantly led by private contractors. Brettmann and NeSmith's (2000-2005) method, developed for augered, pressure-injected drilled displacement piles, can be used with CPT and SPT data alike, and represents the only SPT-based method available in literature for DDPs. As indicated in Table 1, most other methods are derived for drilled or driven piles. Hence their application to DDPs is an extrapolation beyond their intended use, driven by the limited availability of DDP-specific solutions. For instance, two of the most employed SPT based methods (i.e., Decourt (1989; 1995) and Meyerhof (1976)) were derived for driven piles; and O'Neill and Reese (1988) and Brown, *et al.* (2010) are SPT-based methods recommended by the FHWA-NHI-10-016 for drilled shafts.

Table 1. Current SPT & CPT based methods for estimating axial pile capacity

	Pile Type/ Installation	How to determine pile side friction	How to determine pile toe bearing
Direct Methods from CPT data			
Schmertmann and Nottingham (1975-1978)	Driven and Drilled shaft	CPT Sleeve friction (fs) and pile material	CPT Tip resistance qt and over consolidation ratio OCR
deRuiter and Beringen (1979)	Driven piles	Over consolidation ratio (OCR), undrained shear strength (S_u), CPT tip resistance (q_t).	Undrained shear strength Su (Laboratory or CPT), tip resistance qt
LCPC. Bustamante and Gianeselli (1982)	Drilled, driven, grouted, barrettes piles and piers foundations	Eslami's soil classification index, undrained shear strength (S_u), CPT tip resistance (q_t)	Tip resistance qt and pore water pressure u.
Eslami and Fellenius (1997)	Driven piles	Pile construction method and soil behavior type index (I_c)	Tip resistance qt and pile diameter D
Niazi and Mayne (2016)	Drilled piles, jacked piles and driven piles	Sleeve friction (f_s), tip resistance (q_t), soil index behavior (I_c), pile installation, loading direction, loading rate.	CPT Sleeve friction fs, CPT tip resistance, soil index behavior
Brettmann and NeSmith (2000;2005)	Auger Pressure Grouted Drilled Displacement	Soil gradation and angularity, CPT tip resistance (q_t)	Soil gradation and angularity and tip resistance
Bustamante and Gianeselli (1993;1998)	Drilled displacement piles	Pile installation, CPT sleeve friction (f_s), CPT tip resistance (q_t), soil index behavior (I_c)	Sleeve friction, tip resistance, index behavior
Direct Methods from SPT Data			
O'Neill and Reese (1988)	Drilled shafts	Depth below the ground and overburden effective stress	N_{60} blow count, assuming good workmanship
		Adhesion factor and undrained shear strength	Bearing capacity factor and undrained shear strength
Brown, *et al*. (2010)	Drilled shafts	Coefficient of lateral earth pressure before and after construction, overburden effective stress	N_{60} blow count
Decourt (1989; 1995)	Driven and bored piles	Pile installation, soil type, N-index along the pile shaft	Pile installation, soil type, N-index at the pile toe
Brettmann and NeSmith (2000;2005)	Auger Pressure Grouted Drilled Displacement	Soil gradation and angularity and N_{60} blow count	Soil gradation and angularity and N_{60} blow count
Meyerhof (1976)	Bored and driven piles	Shaft coefficient based on the pile installation, N-index along the pile shaft.	Toe coefficient based on the pile installation, N-index at pile toe.

Data Analysis

Database of static pile load tests

Data from more than 50 US-based, and 4 German construction projects was collected. The majority of data originated from the West and South-East of the United States, including California, Florida, and Louisiana as shown in Figure 1. All data was provided by members of the DFI technical committees. The authors performed a comprehensive review of the project information and filtered the projects based on the following:

- Availability of geotechnical site data obtained from high quality in-situ soil testing and sampling; information about the groundwater table location; proximity between in-situ soil test and the DDP location
- Description of the DDP design and construction, including pile diameter, pile length.
- Availability of axial load test data within a meaningful load-displacement range and suitable for failure interpretation.

The need for axial load tests to reach a substantial level of settlement to meaningfully interpret the pile axial failure load resulted in discarding several pile tests from this study. Only load test curves with visible onset of strength loss were kept. These remaining project data are summarized in Table 2, which shows the general site location, number of piles tested at each site, soil type, type of in-situ soil test (e.g. SPT/CPT), pile diameter (D), and pile length (L). The test sites consisted of mostly mixed types of soils with strongly stratified sand, silt, and clay layers. The nominal shaft diameters varied from 35 to 61 cm (14 to 24 inches). The embedment length of the piles ranged from 6 m to 29 m. A total of 129 static axial load test measurements were evaluated against CPT and SPT based predictions (i.e., direct methods). Potential effects of the various types of displacement drilling tools on the piles' axial capacity were not considered in this study, as this information was not consistently available for all projects. This restriction poses a limitation to the study, as the construction method (tool and grout placement) is known to affect the final performance behavior (see Moshfeghi and Eslami, 2018). Nevertheless, is also enabled the authors to conduct a more global performance evaluation without getting involved in proprietary and confidentiality related matters and obtain more data. The asterix (*) in Table 2 denotes sites where pre and post CPT tests were carried out. Post-CPT tests were conducted at a distance ranging from 0.75 to 1.2 m away from the installed pile to assess the potential spatial improvement of the surrounding soil.

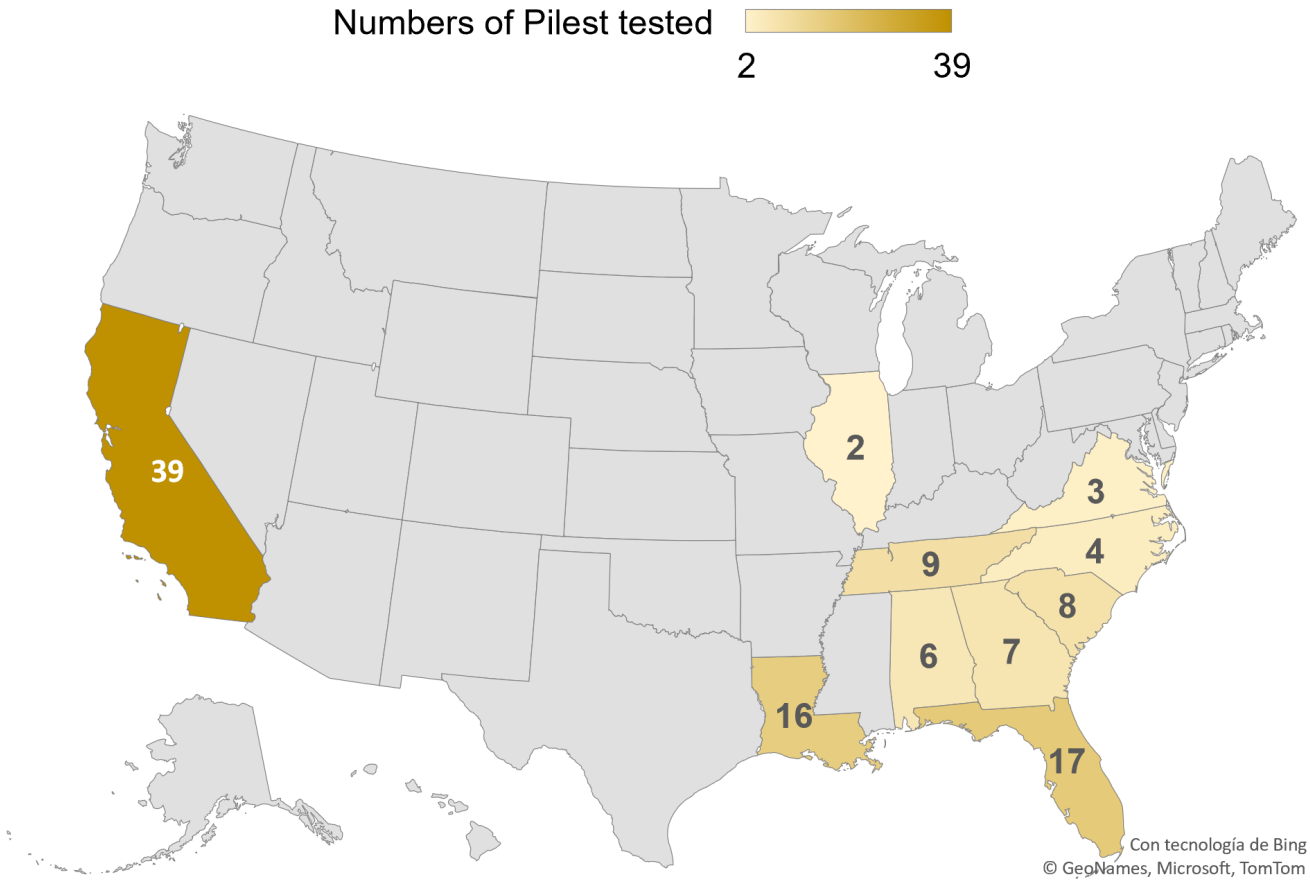

Figure 1. Location of the construction projects in The United States, and number of the piles tested by State

Table 2. Overall information of each project site and tested piles

Location	D (m)	L (m)	Qdesign (kN)	In-situ test	Soil Type	SI	Piles tested
San Francisco, CA	0.45	6.4	427	SPT-CPT	*Silty clay, Clayey silt, silty sand base	3	1
Los Angeles, CA	0.40	8.2	570	SPT-CPT	*Silty clay, Clayey silt, silty sand base	3	1
San Jose, CA	0.40	6.7 - 15.2	214-390	SPT-CPT	*Silty clay, Clayey silt, silt base	3	2
Redwood, CA	0.45	7.6	355	SPT-CPT	*Silty sand, sand, silt, silt base	3	4
Los Angeles, CA	0.40	11.3	1312	CPT	*Sand, silty sand, clayey silt, sand base	3	2
Santa Clara, CA	0.45	14.6	890	SPT-CPT	Clay and silty clay, sand, sandy silt base	3	2
Stockton, CA	0.45-0.60	19.8	667-1000	CPT	Soft clay, sand, stiff clay, silty clay base	2	2
San Francisco, CA	0.40	18.3	1423	SPT	Clayey Silty sand, silty sand, silty sand base	1	1
Anaheim, CA	0.45	13.916.9	1423-2002	SPT-CPT	Silty sand, sand, silt, silt or sand base	3	3
San Francisco, CA	0.45	12.20	1112	SPT	Sand, silty sand, clay, sand base	1	1
Sacramento, CA	0.40	18.9	1112	SPT-CPT	Silty clay, silty sand, sand, silty clay base	2	1
Sacramento, CA	0.45	13.4	890	SPT	Stiff silty clay, clayey silt, sandy gravel base	3	1
San Francisco, CA	0.45	24.3	712.00	SPT	Sandy clay, clay, sand with clay base	3	1
Sacramento, CA	0.35-0.40	23.2	601	SPT-CPT	Silty sand, silty clay, clay, sand, sand base	3	2
San Francisco, CA	0.40	11.3	1120	SPT-CPT	Silty sand, silty clay, sand, sand base	3	1
Sacramento, CA	0.45	10.7-11.6	1334-1912	SPT-CPT	Sand, silty sand, clay, clay base	2	2
Sacramento, CA	0.40	8.2	534	SPT-CPT	Silty sand, silty clay, clay, sand base	3	1
McClellan, CA	0.4	20.4-21.8	569	SPT-CPT	Silty sand, sand, silt, sand base	1	2
Daly City, CA	0.40	21.3	1334	SPT-CPT	Silty sand, sand, sand base	1	1
Santa Rosa, CA	0.45	16.7	667	SPT-CPT	Silty sand, sand, sand base	1	1
Tampa, FL	0.45	7.6	-	CPT	*Sand, silty sand, silt, sand base	1	1
Caddo, LA	0.40	13.4-18.9	1470	CPT	Sand, silty sand, clay, clay base	3	7
Florence, SC	0.35	10.7-14.6	882	SPT	Sand, silty sand, clayey silt, sand base	1	8
Orlando, FL	0.40	13.1-23.2	1225	CPT	Sand, silty sand, clay, sand base	3	7
Guthrie, KY	0.35	13.2-17.8	882-980	SPT	Clay and silty clay, clay base	2	7
Miramar, FL	0.40	8.5-10.1	833	CPT	Sand, silty sand, clayey silt, sand base	1	2
Monroe, LA	0.35	7.9-9.1	980	CPT	Silty sand, silty clay, clay, sand, sand base	1	2
Westlake, LA	0.60	9.1-16.8	490-1323	CPT	Clay and silty clay, clay base	2	3
Mobile, AL	0.40	21.6-24.4	980.00	CPT	Silty clay, silty sand, sand, silty clay base	3	4
Roxana, IL	0.45	6.1-9.8	563-1225	SPT	Sand, silty sand, clayey silt, sand base	1	2
Memphis, TN	0.40-0.45	15.85	421-735	SPT	Clay and silty clay, clay base	2	2
Clayton, NC	0.35	18.3-19.8	1250	SPT	Silty clay, silty sand, sand, silty clay base	1	3
Virginia Beach, VA	0.40	9.5-12.2	735-1176	SPT	Sand, silty sand, clayey silt, sand base	1	2
Atlanta, GA	0.45	10.3-16.5	1960	SPT	Clay and sand, sand base	3	2
Memphis, TN	0.35	7.7-12.9	931	SPT	Sand, silty sand, clayey silt, clay base	1	3
Savannah, GA	0.40	14.0-17.1	1470	CPT	Sand, silty sand, clayey silt, sand base	1	3
Tuscaloosa, AL	0.35	18.6	764	SPT	Sand, silty sand, clayey silt, stiff clay base	3	1
Port Allen, LA	0.35-0.45	9.1-28.9	255-1729	CPT	Clay, silty sand base	3	4
Savannah, GA	0.35	15.9	1112	CPT	Clayey Silty sand, silty sand, silty sand base	3	1
Pensacola, FL	0.40	9.1-11.0	980	SPT	Sand, silty sand, silt, sand base	1	3
Pensacola, FL	0.40	18.29	1274	SPT	Silty sand, silty clay, sand, sand base	1	2

Table 2. Overall information of each project site and tested piles (*Continued*)

Location	D (m)	L (m)	Qdesign (kN)	In-situ test	Soil Type	SI	Piles tested
Mobile, AL	0.40	50.00	-	SPT-CPT	Sand, silty sand, clayey silt, sand base	1	1
Owensboro, KY	0.35	44.00	-	SPT	Silty sand, silty clay, clay, sand, sand base	1	1
Memphis, TN	0.40	50-73	-	SPT	Sandy clay, clay, sand with clay base	1	1
Fort Myers, FL	0.45	75.00	-	SPT	Sand, silty sand, silt, sand base	1	1
Memphis, TN	0.40	70.00	-	SPT-CPT	Clay and silty clay, sand base	3	3
Redwood, CA	0.40	18	711	CPT	Silty clay, sandy silt with medium sand layers	2	2
Redwood, CA	0.40-0.45	18.3	533-711	SPT	Lean and fat clay, and silty sand	2	4
Belmont, CA	0.40	18.3	-	CPT	Soft clay, stiff silty sand and silty clay	2	2
Mountain View, CA	0.40	24.4	-	CPT	Shallow stiff lean clay, and lean clay with sand	2	2
Santa Clara, CA	0.40	23	1140	CPT	High plasticity clay and stiff clay with sand layers	2	3
Kleve, DEU	0.51	9.5-10	-	DPH	Sand, silty sand, sand base	1	2
Glasgow, UK	0.51	13.5	-	CPT	Loose to medium sand, sand base	1	3
Hamburg, DEU	0.35-0.51	5.8-10.3	-	CPT	Medium sand with silt layers	1	4
Rin-Lahn, DEU	0.51	6.5	-	DPH	Sand, silty sand, silt, sand base	1	1

* Projects with Pre and Post CPT
SI: Overall Soil Interpretation. (1) sand like, (2) clay like, and (3) mixed soil

Geotechnical data review

Cone Penetration Test (CPT) and Standard Penetration Test (SPT) data were subsequently processed to obtain geotechnical analysis/design parameters. CPT results were interpreted following Robertson (2015). The SPT N-values (blow-counts/feet) reported in the boring logs were corrected to obtain N_{60} values, based on the sampler method, hammer type, and energy values reported by the respective testing company. SPT results were then further processed using empirical relationships from Hara *et al*. (1974) and Peck *et al.* (1974) to calculate the undrained shear strength and friction angle per Eqs. 1 and 2, respectively, i.e.,

$$S_u = 0.29 P_a (N_{60})^{0.72} \quad (1)$$

$$\phi' = 27.1 + 0.3(N_{1,60}) - 0.00054(N_{1,60})^2 \quad (2)$$

where S_u = undrained shear strength, P_a = atmospheric pressure (101.3 kPa), N_{60} = SPT blow count corresponding to 60% of the theoretical free-fall hammer energy, ϕ' = soil friction angle, and $N_{1,60}$ = energy and overburden pressure corrected SPT blow count.

Most CPT and SPT based design methods require the soil (layers) to be categorized into cohesionless or cohesive soils. Robertson (2015) defines the soil index behavior (I_c) as a function of the CPT based tip and side resistance. A value of I_c higher than 2.6 suggests the soil behavior to be silt like, clayey silt like to silty clay like, or clay-like in general. An I_c value lower than 2.6 suggests sand-like behavior, including silty sands to sandy silts and sands in general. The 2.6 value for the index behavior was employed as a threshold to categorize the soil layers. For the projects in which CPT data were not available, the Unified Soil Classification System (USCS) defined in the SPT logs was utilized for the same purpose. Table 2 categorizes each project location in sand-, clay-, and mixed sites using the I_c criteria described above. Sites with less than 20% of clayey-silt-like index behavior were classified as sandy soil sites. Sites with more than 70% of the clayey-silt behavior index were classified as clayey sites. All other sites were labeled as mixed soil sites. This classification resulted in 23 sandy soil sites; 11 clay sites; and 20 sites with highly stratified soil profiles (mixed soils). Figure 2 shows an example of the in-situ soil test data and an accompanying axial load-settlement curve (Figure 3) for a project located near Redwood, CA. This site would be categorized as mixed site since 55% of the calculated soil behavior indices (SBT) along the pile depth reach values higher than 2.6 (suggesting clayey soil), and 45% of the SBT indices are lower than 2.6 (suggesting sandy soil). Four piles were axially tested on this site, and Figure 3 shows the results for every pile (A, B, C, D). Pile A and C revealed clear plunging behavior (increase of settlement higher than 20% due to an 2% increase of axial load) at an axial load of 910 kN and 1230 kN, respectively. For piles B and C, the plunging behavior cannot be clearly observed. The maximum increase of settlement due to an increase of axial load of 2%, was recorded as only 9% and 5% for each pile, respectively.

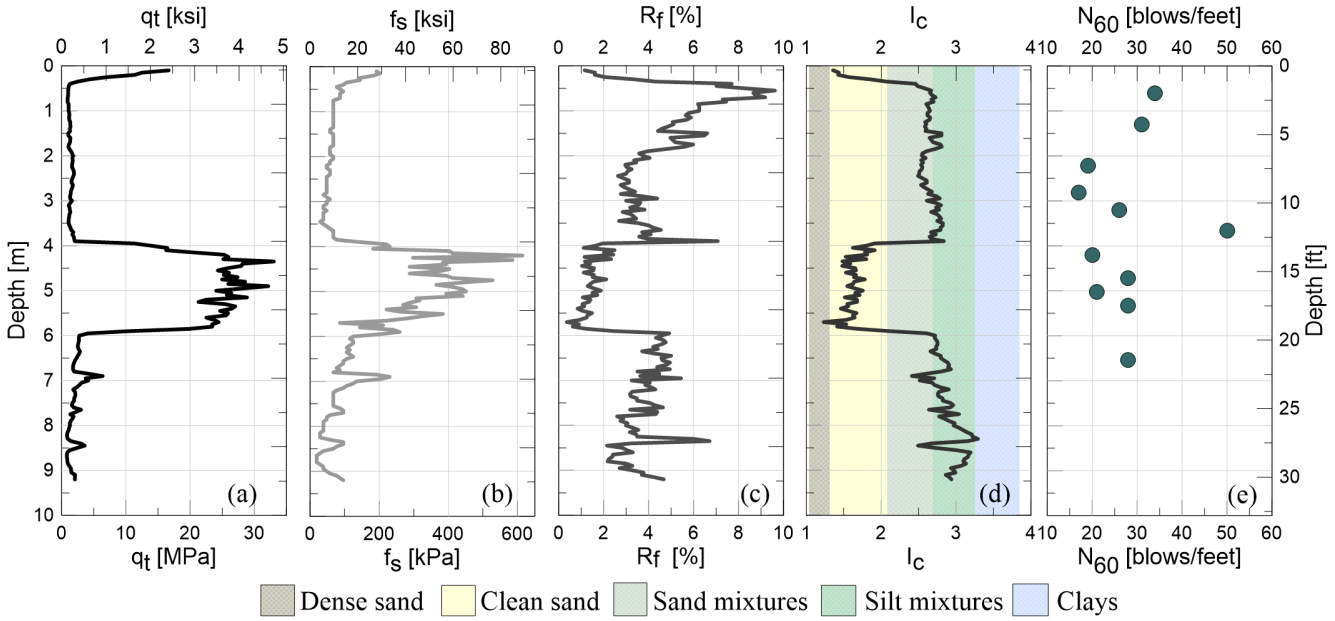

Figure 2. Example: Redwood city project in-situ soil test: (a) CPT tip resistance (qt). (b) CPT side resistance (fs). (c) Friction ratio R_f in %. (d) Soil index behavior (I_c) per Robertson (2015). (e) Energy-corrected SPT blow counts N_{60}

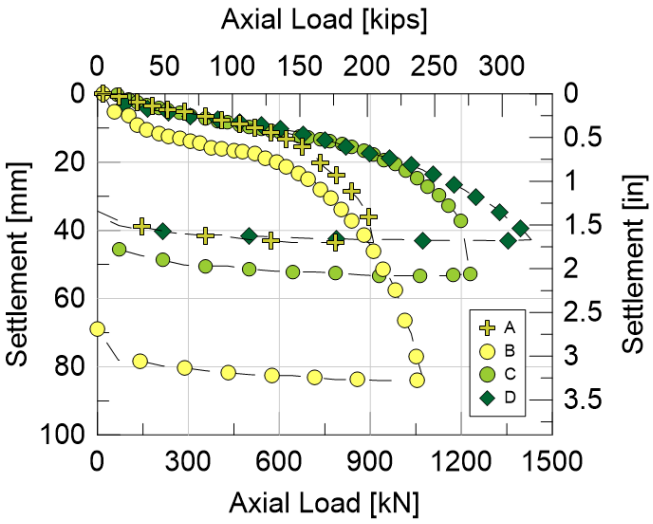

Figure 3. Axial load-settlement curve from test

Interpretation of axial failure based on pile load tests

The American Society for Testing and Materials (ASTM, 2020), as well as the American Association of State Highway and Transportation Officials (AASHTO, 2008) define the failure load as the load which induces a visually observable plunging behavior in the axial load versus displacement curve. The plunging behavior is referred to as a gross settlement of the tested element. In turn, Fellenius (2001) highlights the fallacy and misinterpretation of the "failure load" or "ultimate load" of a pile since the shaft resistance is the only resistance mechanism that exhibits a limiting resistance while the axial compression of the pile and the pile toe bearing show a linear response and do not have an ultimate value besides the structural failure of the pile. As an alternative, Fellenius (2001) suggests the use of the load that triggers a settlement equal to 10% of the diameter of the pile. The International Building Code (IBC), 2019, defines the allowable pile load as one half of the ultimate axial load of the test element assessed by using Davisson Offset Limit, Brinch-Hansen 90% criterion, Butler-Hoy criterion, and other methods approved by the building official.

For piles in soft or medium clays, plunging behavior can be clearly identified in most load-settlement curves; therefore, failure loads can be easily determined through visual inspection. On the other hand, for medium soils, stiff clays, and sands, the slope of the resulting curve is stiffer and does not necessarily show the change in the slope during loading (i.e., it does not reach failure). Amongst the projects collected for this study, eight axial load tests were discarded due to the very flat load-displacement curve during the test (e.g., pile-soil system is too stiff) such that no tendency towards failure can be identified within the available range of test data. Regardless of the soil conditions, geotechnical failure generally occurs well before the ultimate structural capacity of the pile is reached.

To determine the failure load for each project listed in Table 2, two different approaches were adapted: (i) failure was defined based on substantial strength loss (plunging) whenever clearly visible in the vertical load vs. displacement curves: this was the case for 30 piles, and (ii) failure loads were estimated using interpretation methods from literature whenever failure was not reached experimentally (which was performed for 70 piles). Additionally, a corresponding axial load for a settlement equal to 10% of the pile diameter was identified whenever possible.

Review of existing methods to interpret axial pile failure

Current literature offers several methods to estimate/interpret the anticipated failure load when axial failure was not reached during field testing. The most common approaches are Decourt Extrapolation (1999), the Davisson Offset Limit Load (DOL) (1972), the Hansen 80-% Criterion, the Brinch-Hansen 90% criterion, Chin-Kondner Extrapolation (1970) also known as the inverse method, the Butler & Hoy (1977) Load, also known as "double tangent method" or "L1-L2 method", De Beer's Criterion (1968) or "maximum curvature" method, and the Van der Veen's Criteria (1953). The corresponding axial load for a settlement equal to 10% of the pile diameter was defined as an alternative "failure load" for CPT methods such as the Niazi and Mayne (2016) and Bustamante and Gianeselli (1993; 1998) methods, which define the predicted failure load at a displacement equal to 10% of the pile diameter instead of the traditional definition of pile failure in literature.

The procedure to identify the failure load for each of the above-listed methods is described hereafter. Figure 4 summarizes these methods graphically, by depicting the required tangents and bisectors to a schematic load-displacement illustration.

Decourt Extrapolation (Decourt, 1999)

The measured values from the axial load test are assumed to be hyperbolic and required to be fitted by Equation 3. Once the values calculated with Equation 1 fit the observed data, the failure load is determined by the inverse value of the fitting constant k_2, i.e., $Q_f = 1/k_2$.

$$Q = \frac{\delta}{k_1 + k_2 \delta} \tag{3}$$

Where Q is the applied axial load, δ is the pile settlement, and the values k_1 and k_2, are fitting constants to the hyperbolic equation found by using ordinary square regression.

The Davisson Offset Limit Load (DOL) (Davisson, 1972)

Widely used in North America, this method defines the ultimate failure load as the load corresponding to a settlement equal to the elastic compression of the pile (δe) (Equation 4) plus the sum of settlements required to mobilize the shaft and the tip resistance. The authors believe that the maximum shaft and tip resistance is achieved at a settlement equal to the sum of 3.8 mm (0.15 inches) plus a settlement equal to the pile diameter, in inches, divided by 120.

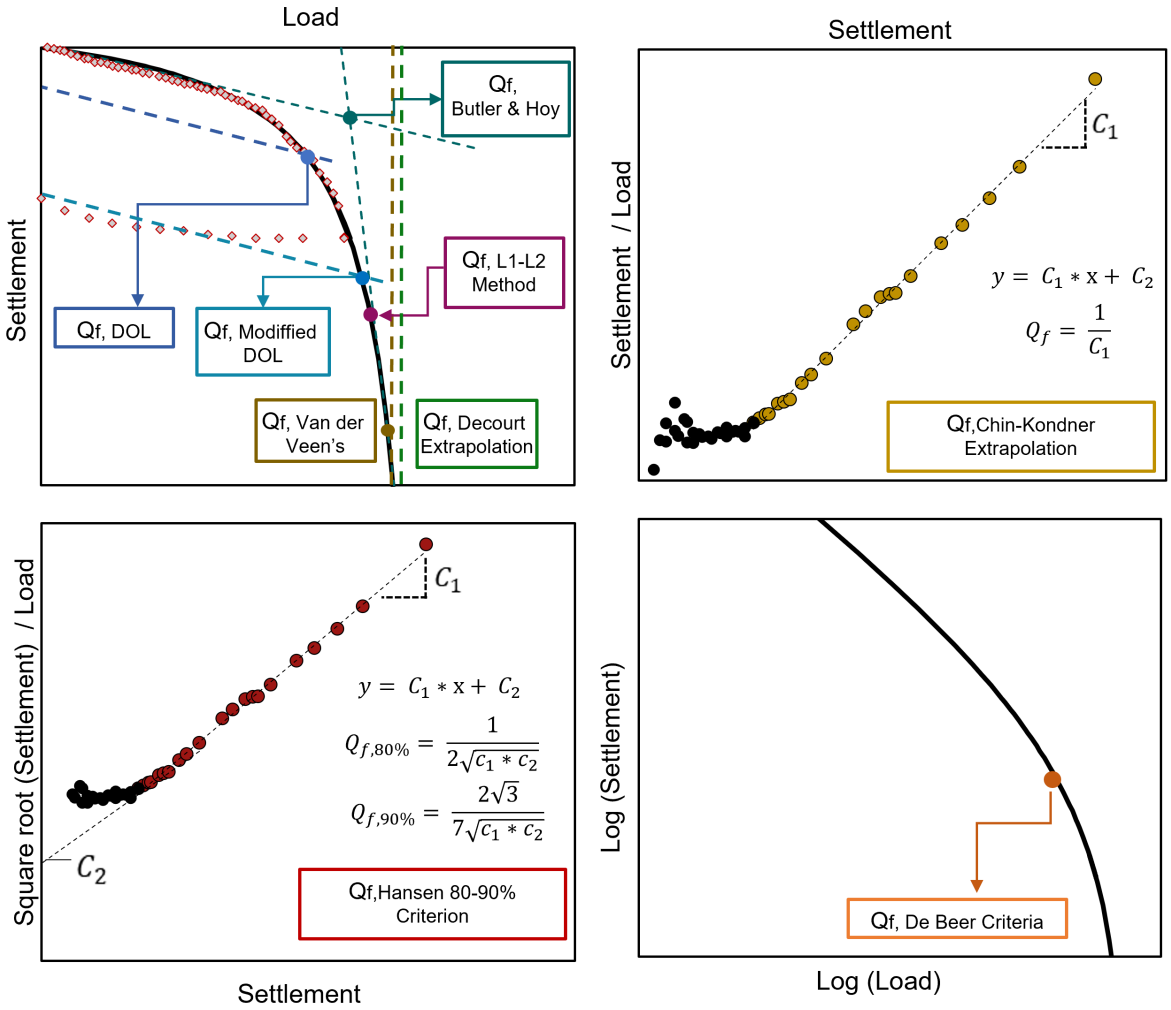

Figure 4. Illustration of the interpreted failure load methods for the static-axial load test

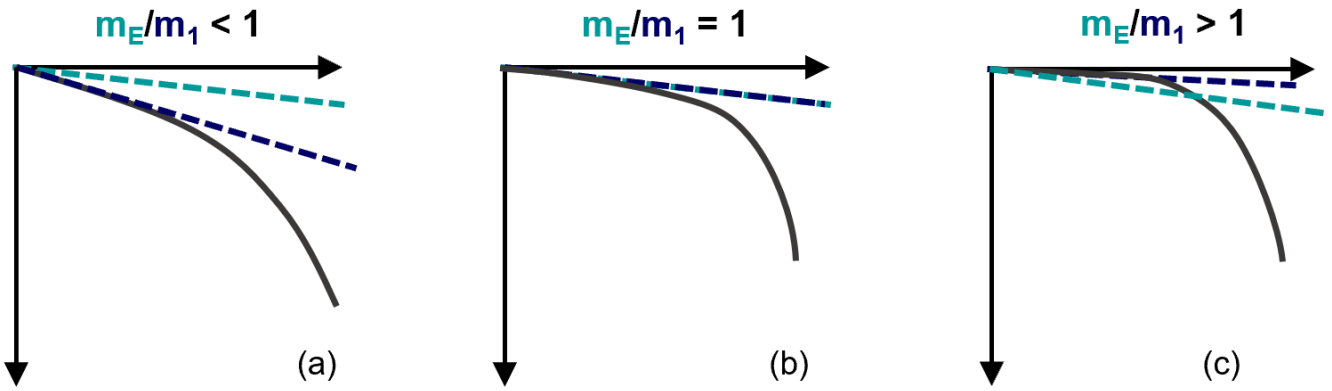

Figure 5. m_E/m_1 diagram

$$\delta e = QL/AE \quad (4)$$

$$\delta = \frac{QL}{AE} + 3.8 \text{ mm} + D[\text{in}]/120 \quad (5)$$

Hereby, Q is the test load, A is the transverse area of the pile, and E is the elastic modulus based on the compressive strength of the concrete grout utilized to construct the piles. The interpreted failure load ($Q_{f,int}$) is defined as the intersection [δ_{int}, $Q_{f,tint}$] of the offset line, δ calculated at different levels of axial load (Q), and the load-settlement curve obtained during the axial load test.

Even though the Davisson Offset Limit Load (1972) is one of the most-used failure interpretation method in practice, its accuracy is strongly dependent on the pile installation technique and is often extrapolated beyond its applicability for driven piles. Hence, its use is heavily critiqued within the deep foundation community. For instance, Stuedlein *et al.* (2014) performed a similar study as presented in this paper, assessing a set of failure load interpretation methods to determine their suitability for augered cast in place piles (ACIP piles), and suggested the Davisson Offset Limit Load to be inappropriate for drilled foundations. This agrees with plentiful discussion in literature showing that the DOL method underestimates the failure load (NeSmith and Siegel, 2009, Baligh and Abdelrahman, 2005-2006, Stuedlein *et al.*, 2014). The difference between the interpreted failure load obtained with the DOL method and the actual failure load is attributed to two factors, namely (1) the slope of the initial straight line of the axial load test (m_1) does not always represent the slope (m_E) that the elastic axial load deformation would have per Equation (4); and (2) the soil quake deformation (third term of Equation 5) to mobilize the soil strength is higher for drilled foundations than the deformation needed for driven piles. To address this issue, Perlow (2020) studied the soil quake factor of the DOL method (i.e., D/120), finding that the pile width needed to calculate the soil quake deformation, should be multiplied by a factor ranging from 2 to 6 depending on the drilled foundation type (i.e., drilled shafts, cased micropiles, drilled displacement piles, among others). This adjustment enables a better estimate for drilled shaft failure loads when using the Davisson Offset Limit Load method.

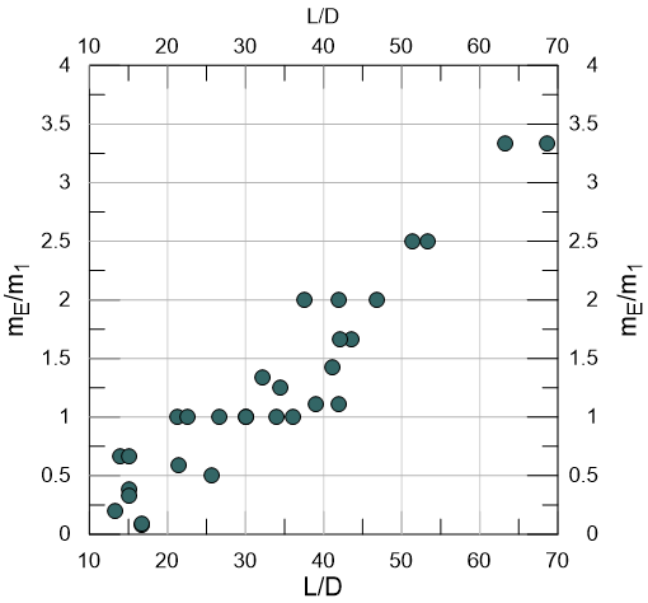

Figure 6. m_E/m_1 values vs. pile slenderness

From the DDP data collected in this study, 30 axial load tests showed a clear plunging behavior, and were used to evaluate the limitations of the DOL method with respect to drilled displacement piles. Since the uncertainty of the DOL method is associated with the discrepancy between the slope of the first line of the test results (m_1) and the elastic slope (m_E), the ratio between these two lines (k) was obtained for each test using Equation (6). As shown in Figure 5, when m_E/m_1 is less than one, the pile settlement is higher than the elastic deformation for small loads (Equation 4), on the other hand, when the ratio is higher than one, the initial axial deformations are lower than the amount of elastic deformation expected. Figure 6 shows the ratio k versus the piles' slenderness ratio L/D. For slender piles, L/D higher than 20, the initial settlement of the pile is not shown at early stages (shaft is effectively resisting the dragging forces). On the other hand, m_E/m_1 lower than one demonstrates how the pile settlement starts developing at earlier stages.

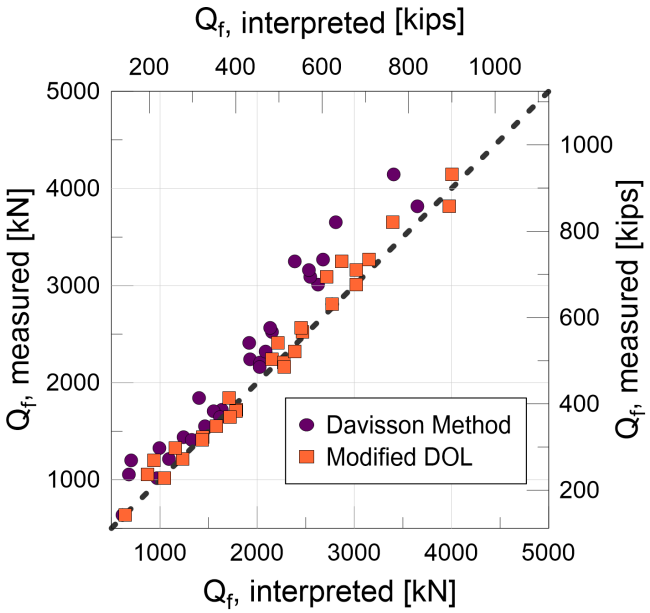

Figure 7. Comparison of the measured (geotechnical failure) and predicted failure load with the DOL and the MDOF methods

$$k = \frac{m_E}{m_1} \tag{6}$$

where m_E is the elastic slope, and m_1 is the slope of the first line from the axial load test.

Following Perlow (2020), the DOL method was modified by applying an amplification factor of 4 to the soil quake deformation (third term of the DOL equation – Eq. 5). Figure 7 shows the comparison between the measured failure load vs. the interpreted failure load estimated with Davisson Offset Limit Method (DOL) and Modified Davisson Offset Limit (MDOL). The MDOL data points align better to the 45-degree line which represents the perfect agreement between the measured and the interpreted failure load. The ratio between experimental and the interpreted axial failure load was obtained for the piles that reached the geotechnical failure while testing. The μ value represents the average ratio for all piles and σ represents the standard deviation. The MDOL method shows a 12% increase in accuracy compared to the original DOL method. The standard deviation of the ratio between the interpreted failure load $Q_{f,interpr}$ using the modified DOL and the measured failure load $Q_{f,measured}$ in the field, as introduced later in this paper, reduced by 30%, showing less scatter amongst results when comparing interpreted failure with the actual failure load obtained during the test.

Brinch Hansen 80% Failure Criterion (Hansen, 1963)

The Brinch-Hansen 80% criterion suggests the failure load to be reached at the level of compressive stress (Q/A) at which the axial strain in the pile is equal to four times the strain at a 20% smaller stress. This concept was translated by Dotson (2013) into a direct solution that requires plotting the square root of each pile displacement value normalized by its corresponding load plotted against the respective pile settlement. Hereafter, a trendline with slope C_1 and intercept C_2 is fitted to the plotted data. The Hansen 80% criterion defines the failure load as the inverse value of two times the square root of C_1 times C_2 as shown in Equation (7).

$$Q_u = \frac{1}{2\sqrt{c_1 c_2}} \tag{7}$$

Brinch-Hansen 90% criterion (Hansen -1963)

The Brinch Hansen 90% criterion interprets pile failure as the load for which strain is equal to two times the strain at a 10% smaller stress. Similar to the 80% criterion, Dotson (2013) proposed a direct solution of the failure load obtained with the 90% criterion as shown in Equation (8),

$$Q_u = \frac{2\sqrt{3}}{7\sqrt{c_1 c_2}} \tag{8}$$

where Q_u represents the interpreted failure load, and C_1 and C_2 are the slope and the intercept of the linear tendency defined for the Hansen-80% criterion.

Chin-Kondner Extrapolation (Chin, 1970)

To apply the Chin-Kondner Extrapolation method, a plot of the pile settlement measured during the axial load test (x-Axis) vs. settlement divided by its corresponding load (y- axis) needs to be constructed (Figure 4). A trendline is fitted to the data above ($y = C_1x + C_2$), its slope is defined as C_1 and its y-intercept as C_2. The failure load is calculated as the inverse of the trendline's slope, i.e., $Q_f = 1/C_1$.

Butler-Hoy Criterion (Butler and Hoy, 1977)

The interpreted ultimate failure load is defined as the point of intersection between a line fitted to the initial straight part of the load-settlement plot, and a second line with a pre-defined slope of 0.13 mm/kN (0.05 in/ton). This second line is to be placed at the point of minimum curvature in the pile's load-settlement curve.

L1-L2 method (Hirany and Kulhawy, 1989)

The interpreted failure load is defined based on the points L_1 and L_2, where L_1 represents the "end point" of the initial straight-line portion of the pile load-settlement curve, and L_2 represents the first point of the final linear region. L_2 simultaneously defines a failure threshold, as any incrementally small load beyond point L_2 produces a significant increase in pile displacement. Q_{L1} and Q_{L2} are the loads corresponding to points L_1 and L_2, respectively.

De Beer Yield Load (De Beer, 1968)

The pile load test data is plotted on a log scale of the measure load (Q), and a log scale of the settlement (δ) (Figure 4). If the plunging behavior was reached during testing, two consecutive lines approximations will show. The point where the lines change their direction, or the maximum curvature of the plot is interpreted as failure load or yield load as defined by the authors.

Van der Veen's Criteria (Van der Veen, 1953)

The measured values from the axial load test are assumed to fit an exponential relationship shown by Equation 9, where Q_u is the interpreted failure load, δ is the in-situ settlement, and β represents a curve fitting parameter. Q_u and β can be found by using ordinary square regression. Q represents the axial load at any point along the exponential curve.

$$Q = Q_u(1 - e^{\frac{-\delta}{\beta}}) \quad (9)$$

To date, there is no established best practice in selecting the appropriate interpretation method. Stuedlein *et al.* (2014) found pile failure of Auger Cast Piles to be best interpreted with the Butler & Hoy (1977) and L_1-L_2 methods. The Davisson method is widely known for its application and validity for small-diameter driven piles, and although the criteria was originally developed for tip bearing driven piles, it has been proven that it can also be utilized for driven friction piles (NeSmith and Siegel, 2009). However, similar to the earlier-described predictive equations for axial pile capacity, extrapolation of formulations beyond their original empirical development is generally recommended against. For drilled displacement piles, no such relationship has been established yet. Hence, a preliminary assessment of the interpretive failure load methods was carried out to identify the methods that best describe the failure load of DDPs included in this study. First, all failure interpretation methods listed above were applied to 30 DDP tests during which experimental failure was reached and the corresponding failure load is known. Similarly, all tests for which a settlement equal to 10%D was obtained, were included. Hereafter, the ratio of interpreted failure load ($Q_{f,int}$) and actual, measured failure ($Q_{f,meas}$) was calculated. The best-performing interpretation method was defined as the one with an average ratio closest to one (1.0) and minimal standard deviation for all tests considered. A normal distribution was calculated to assess the accuracy and precision of the methods. Figure 8 shows the Probability Density Function (PDF) of the normal distribution calculated for each method and suggests the Van der Veen's Criteria (1953) to provide the closest match and most accurate estimate of the actual failure load, followed by Butler and Hoy (1977), and the L_1-L_2 method. Both, De Beer's Criterion (1968) and the DOL Method, underestimates the failure load of the piles, and the Decourt Method and Chin-Kondner Extrapolation overestimate the failure load. Even though the L_1-L_2 method shows good predictive performance of the failure load, a significant number of assumptions are needed when load test data don't reach the magnitude of settlements needed to establish the second "linear" portion of the load-settlement curve. Finally, the interpreted failure load at settlement equal to 10% of the pile diameter (i.e., 0.1D) was estimated based on the axial load – settlement data. Even though the 10%D approach closely approximates the measured failure, this criterion had to be discarded since not enough load tests reached this level of settlement, which is common particularly for piles with large diameters. Figure 9 summarizes the load ratios obtained through all methods in a single graph. Based on this summary, Van der Veen's criteria (1953) was found to be most suitable and consequently applied to all tests that did not reach failure in order to inter-

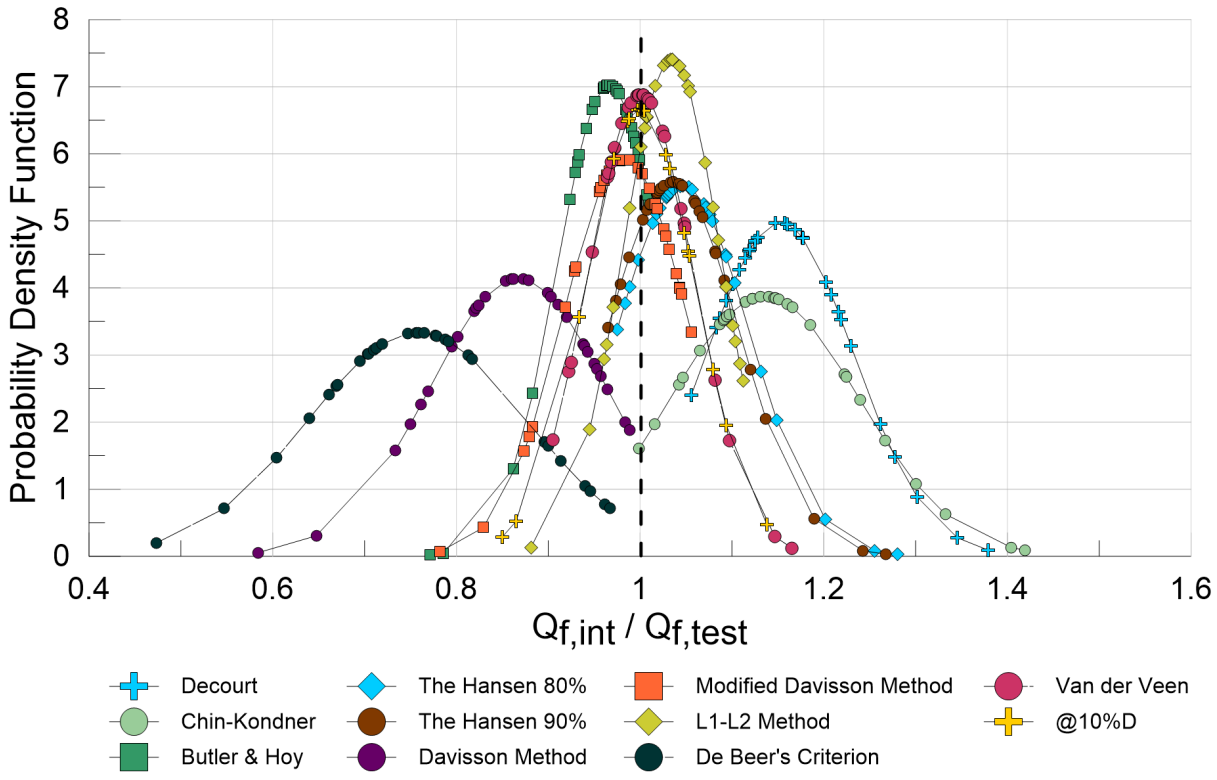

Figure 8. Probability density function for the $Q_{f,int}/Q_{f,test}$ ratio of each interpretation method

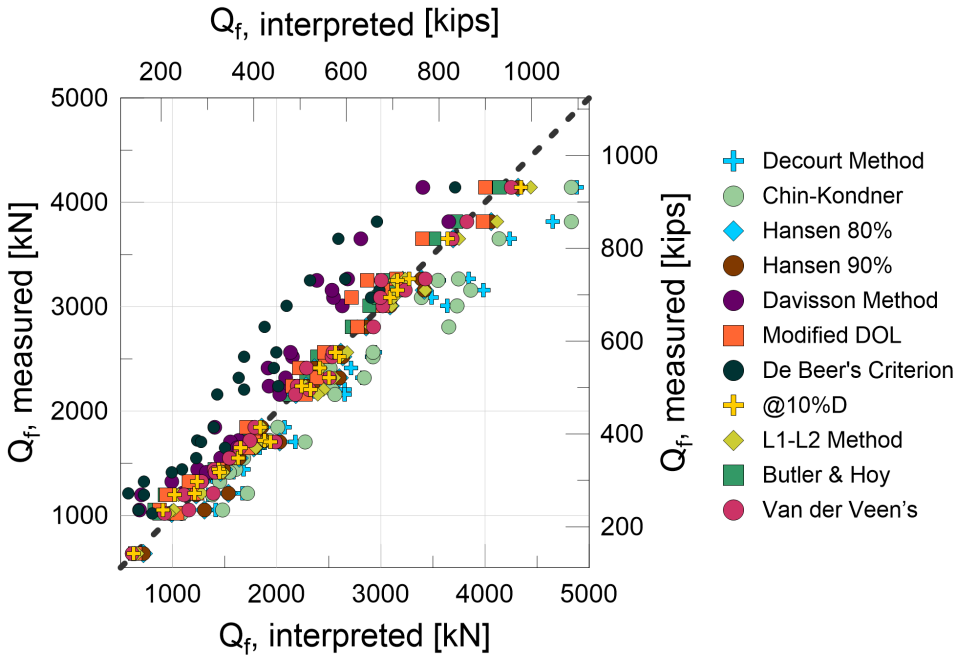

Figure 9. Comparison of the measured (plunging failure) and predicted failure load

pret and estimate the anticipated pile failure load, hereafter referred to as $Q_{f,interpreted}$.

Data Analysis

The accuracy of each available direct method in predicting pile axial capacity was assessed by calculating the ratio between the measured experimental axial failure load (Q_f) and the analytically predicted (i.e., calculated) axial capacity (Q_c) for each pile specimen listed above. The axial failure load was either taken as the measured load at failure ($Q_{f,measured}$) or the interpreted load ($Q_{f,interpreted}$) per Van der Veen's Criteria (1953) when plunging behavior was not observed experimentally. 100% predictive accuracy is reached when the ratio of failure load divided by the predicted load is one. The arithmetic mean (μ) and the standard deviation (σ) were calculated according to Equation 10 and Equation 11. The confidence limit (CL) was also calculated for the ratio Q_f/Q_c based on Equation 12, where Z is equal to 1.96 for a 95% confidence limit according to Hogg and Craig (1995). The Confidence Interval (CI) Equation (Equ.13), represents the range in which 95% of the mean of the samples will fall. The results for Q_f/Q_c are presented in Figure 10 for sand, in Figure 11 for clay and in Figure 12 for mixed types of soils. An optimum result is defined by a mean value (μ) near unity and a minimal standard deviation to assure the trend (ratio of under or over prediction) with a higher precision. The CPT direct methods are shown with round symbols, and the SPT results with square symbols.

$$\mu = \frac{\sum_{i=1}^{n}\left(\frac{Q_{f,i}}{Q_{c,i}}\right)}{n-1} \tag{10}$$

$$\sigma = \frac{\sum_{i-1}^{n}\left(\frac{Q_{f,i}}{Q_{c,i}} - \mu\right)^2}{n-1} \tag{11}$$

$$CL = \mu \pm Z \times \frac{\sigma}{\sqrt{n}} \tag{12}$$

$$CI : \left[\mu - Z \times \frac{\sigma}{\sqrt{n}}, \mu + Z \times \frac{\sigma}{\sqrt{n}}\right] \tag{13}$$

Figure 10 suggests that measured and analytically predicted capacities (i.e., Q_f/Q_c) in sandy soils reach closest agreement when using Brettmann and NeSmith (2000; 2005) and Schmertmann and Nottingham (1975;1978) to calculate the pile axial capacity. De Ruiter and Beringen (1979), LCPC (1982), and Niazzi and Maine (2016) were found to almost exclusively underpredict the in-situ pile capacity in sands, implying a strong conservatism when applied for drilled displacement piles. On the other hand, Eslami and Fellenius (1997) and Bustamante and Gianeselli (1993; 1998) were found to yield axial load capacities 1.25 times higher than what the measured or interpreted results show. By comparing SPT-based methods with the measured or interpreted failure load, the O'Neill and Reese (1988) method showed slightly better alignment with the 45 degrees line than other methods, even though a high dispersity is visible. Figure 10 suggests that the Brown *et al.* (2010), and Meyerhof (1976) methods tend to generally underestimate the in-situ capacity of the piles. Decourt (1989; 1995) show uniform datapoints on both sides of the spectrum (under and overpredicting), with larger

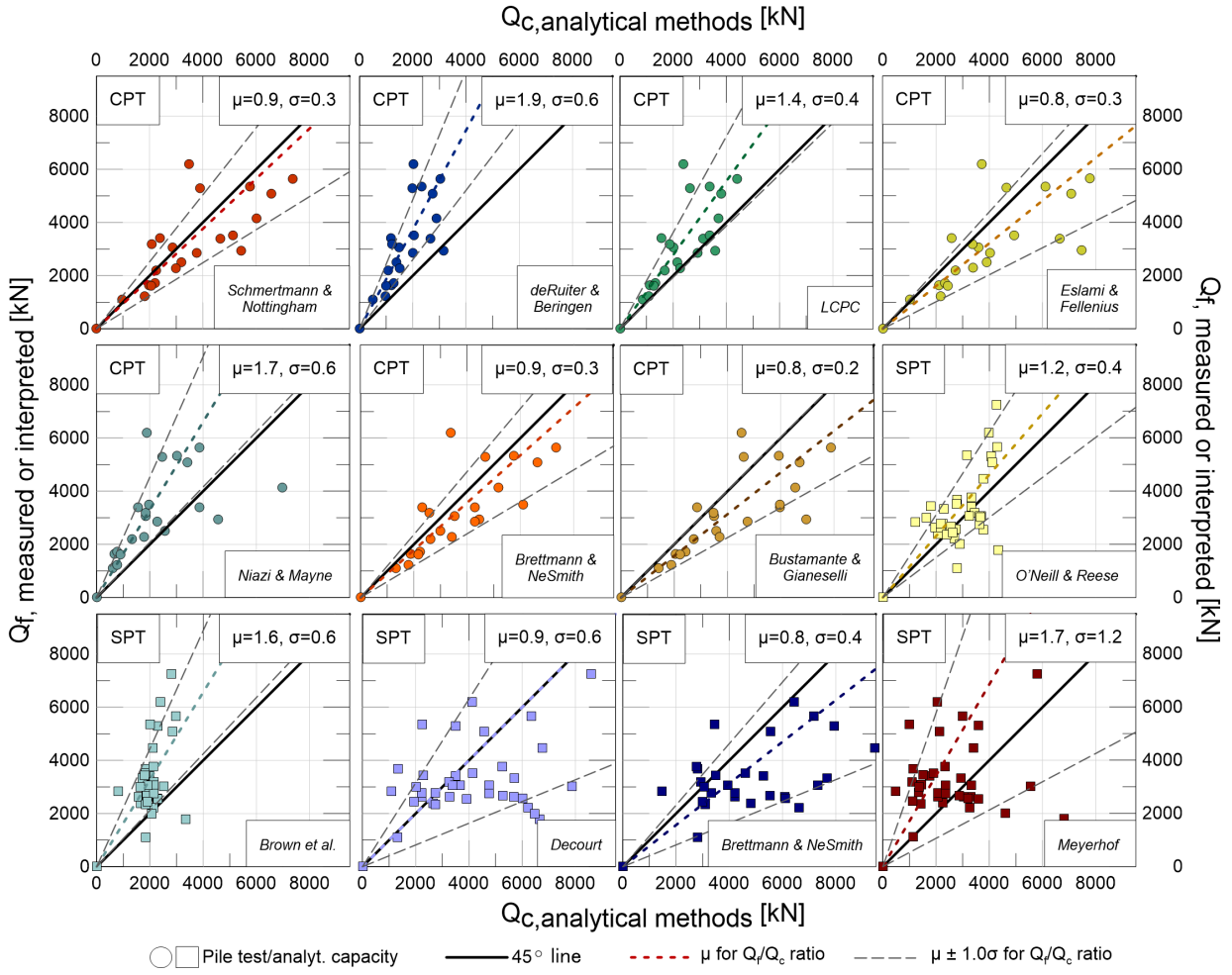

Figure 10. Measured or interpreted failure load versus the axial load capacity estimated analytically from the CPT (point symbol) and SPT (square symbol) direct methods for sandy soils

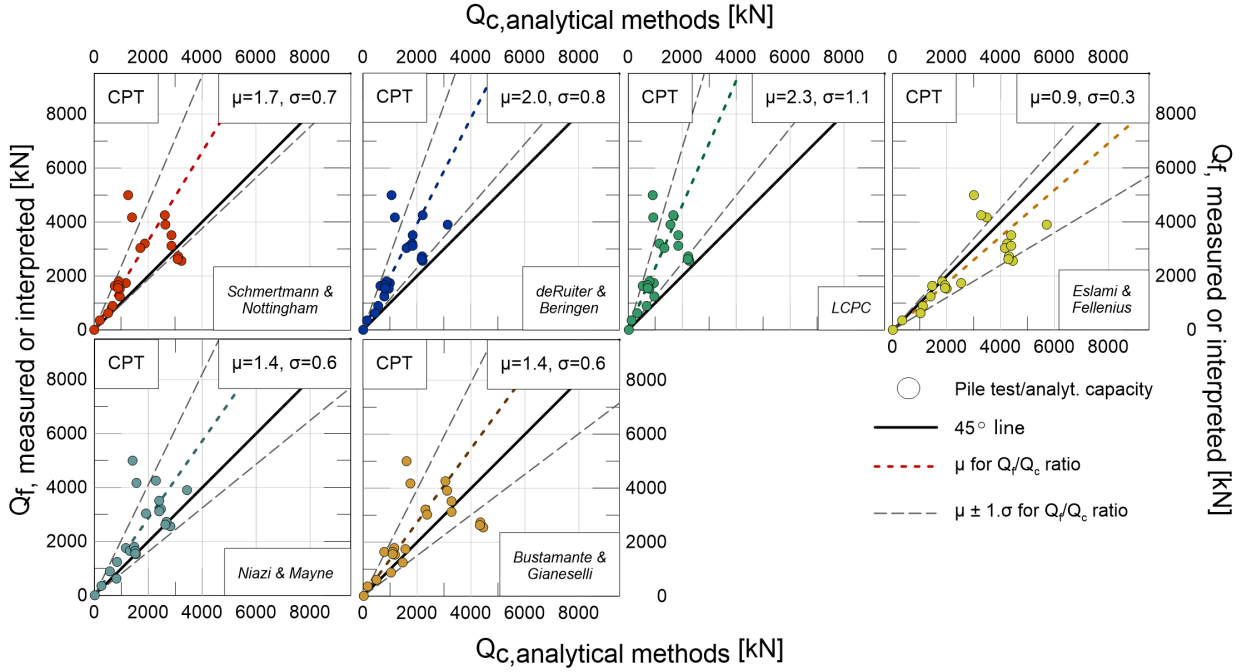

Figure 11. Measured or interpreted failure load versus the axial load capacity estimated analytically from the CPT (point symbol) for clayey soils

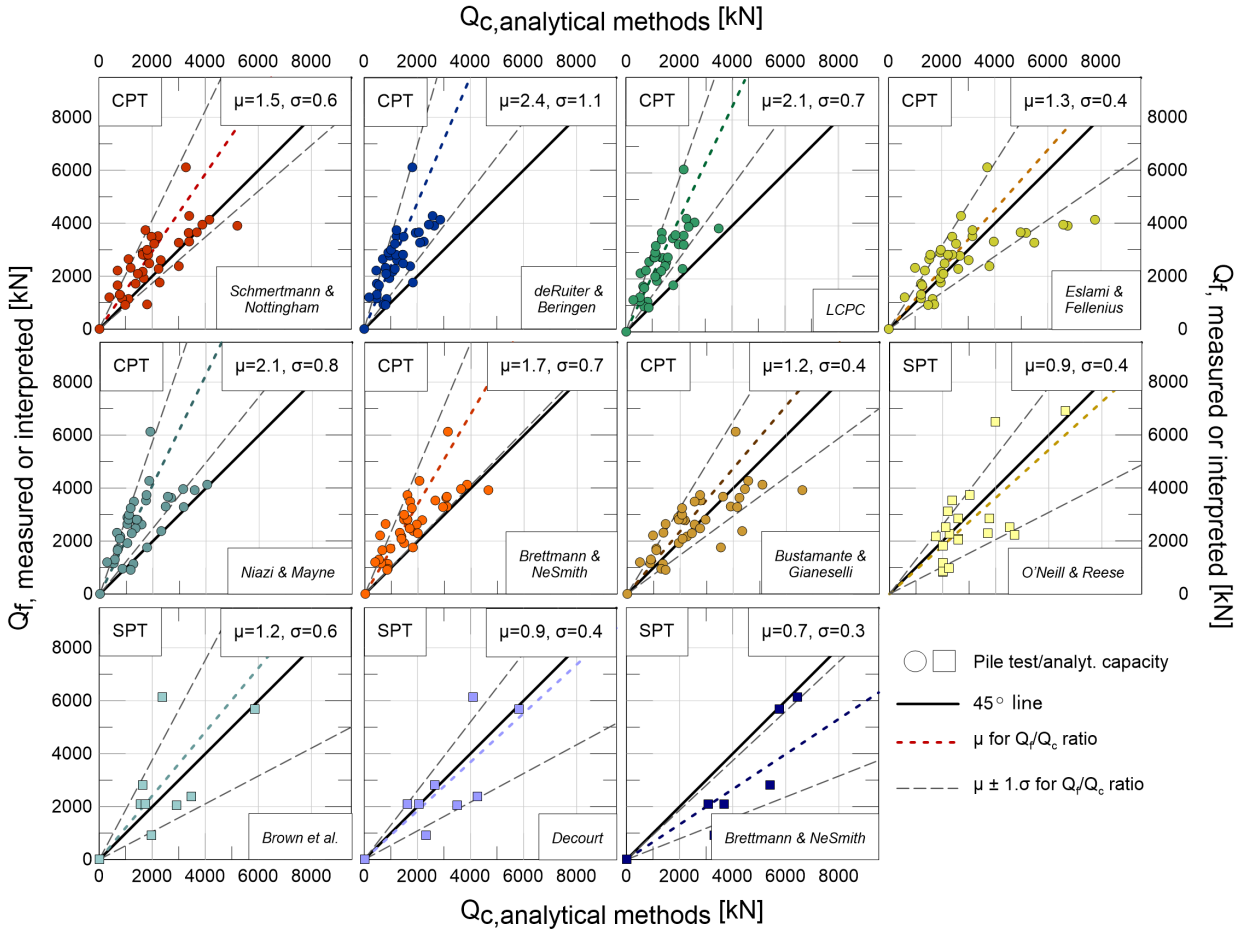

Figure 12. Measured or interpreted failure load versus the axial load capacity estimated analytically from the CPT (point symbol) and SPT (square symbol) direct methods for mixed type of soils

variability. Brettman and Nesmith (2000; 2005) appears to overpredict the capacity when N_{60} values are used to calculate the axial load capacity.

Figure 11 presents the comparison of Q_f/Q_c in clayey soils. For axial loading below 2000kN (450 kip), all methods align well with the CPT-based predictions. Above this load threshold, most methods tend to significantly underestimate the actual capacity of the elements. The Eslami and Fellenius method appears to provide the best statistical fit regardless of the magnitude of axial failure load, however, the favorable statistical results are likely due to an even scatter above and below the 45-degree line. Due to the absence of SPT field data for load tests in clayey soils, the analytical SPT methods could not be assessed.

Figure 12 shows measured vs. analytically predicted pile capacities for mixed soil profiles. Data points for most CPT methods suggest very consistent predictions (very small scatter for most methods). Within the CPT-based methods, Bustamante and Gianeselli (1993; 1998) provide the best approximation of the pile failure load in mixed soils, followed by Eslami and Fellenius (1997). De Ruiter (1979), LCPC (1982), Niazi and Mayne (2016), as well as Brettman and NeSmith (2000; 2005) conservatively underpredicted the field capacity. The O'Neill and Reese (1988) method provides the closest predictions when SPT data is utilized.

Figure 13 shows the mean values and confidence interval for the ratio Q_f/Q_c for the different soil types and analytical methods. The more accurate the method is, the closer is the mean value (circular mark) to one, accompanied by a small confidence interval (shorter vertical line). As it can be seen in Figure 13, the ratio Q_f/Q_c exhibits the highest variability and largest confidence intervals for clayey soils.

Figure 14 and Figure 15 display a comprehensive comparison between all experimental failure loads (measured and interpreted) (y-axis), and their respective, analytical predictions using all methods (x-axis) combined into one single graph. The three symbol types (e.g., square, circle, and triangle) categorize the results into sandy soils (square), clayey soils (circle), and the mixed soils (triangle) from CPT (Figure 14) and SPT (Figure 15), respectively. A global comparison of all CPT-based methods suggests a general underestimation of the pile failure loads, while SPT based methods tend to underestimate the axial load capacity often.

To study the influence of pile geometry on the Q_f/Q_c ratio, the pile slenderness ratio, defined as L/D was computed for each pile (*where* L represents the total pile length and D defines the pile diameter). The L/D ratio was plotted versus

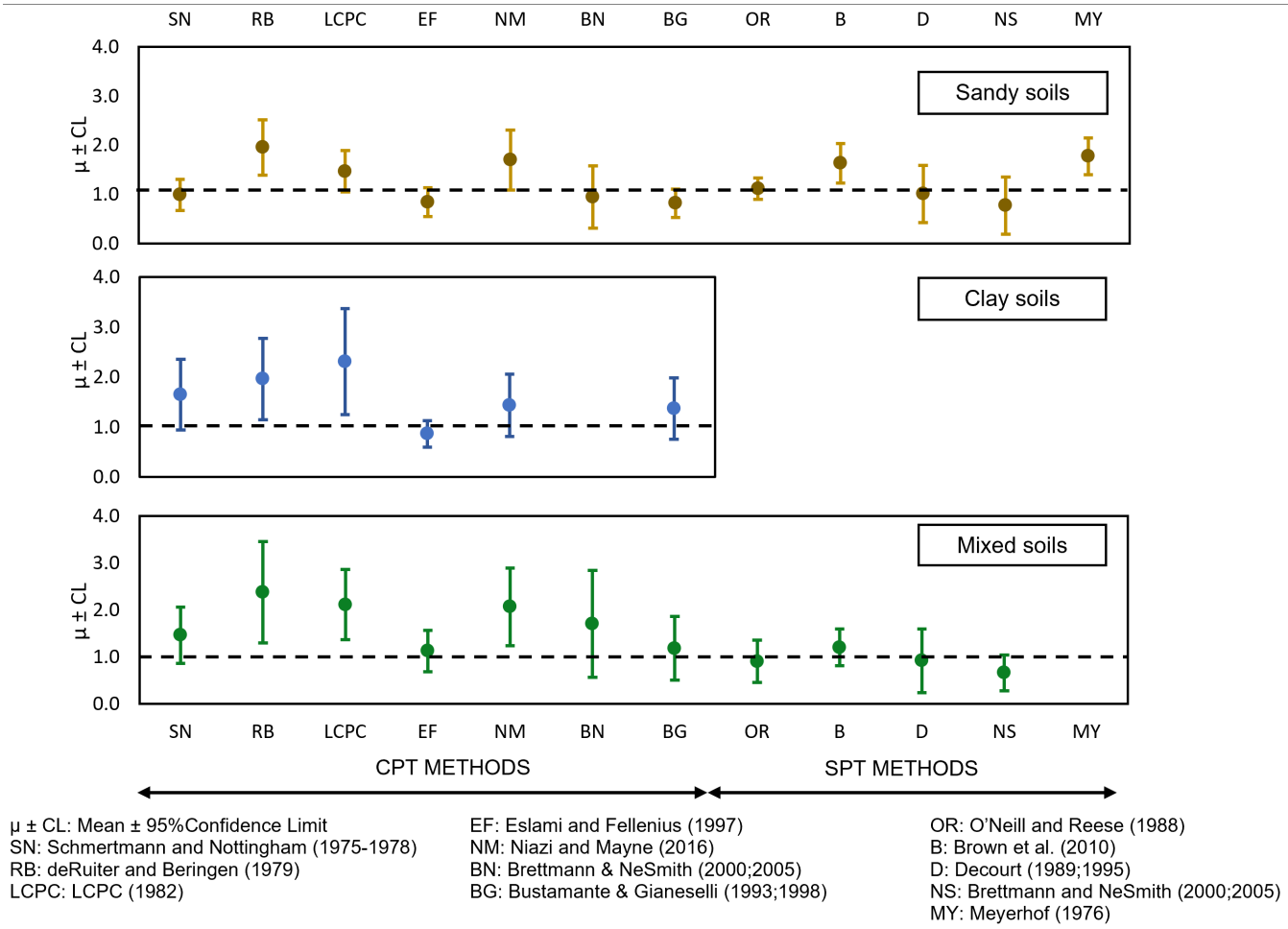

Figure 13. Arithmetic mean (dot mark), and upper and lower confidence bounds (vertical line) for the ratio "Measured or interpreted failure load" over the axial load capacity estimated analytically from the CPT and SPT direct methods

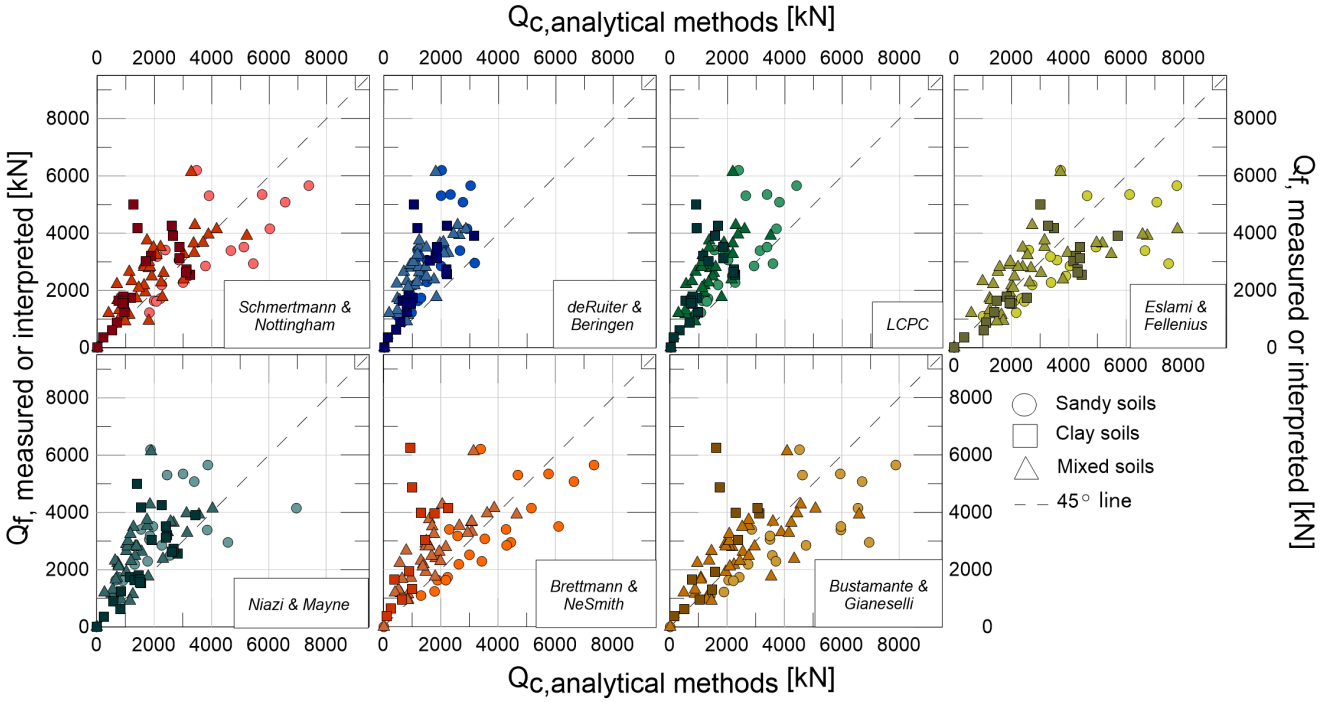

Figure 14. Interpreted failure load versus the axial load capacity estimated analytically from the CPT methods (Data from all soil types plotted in one graph)

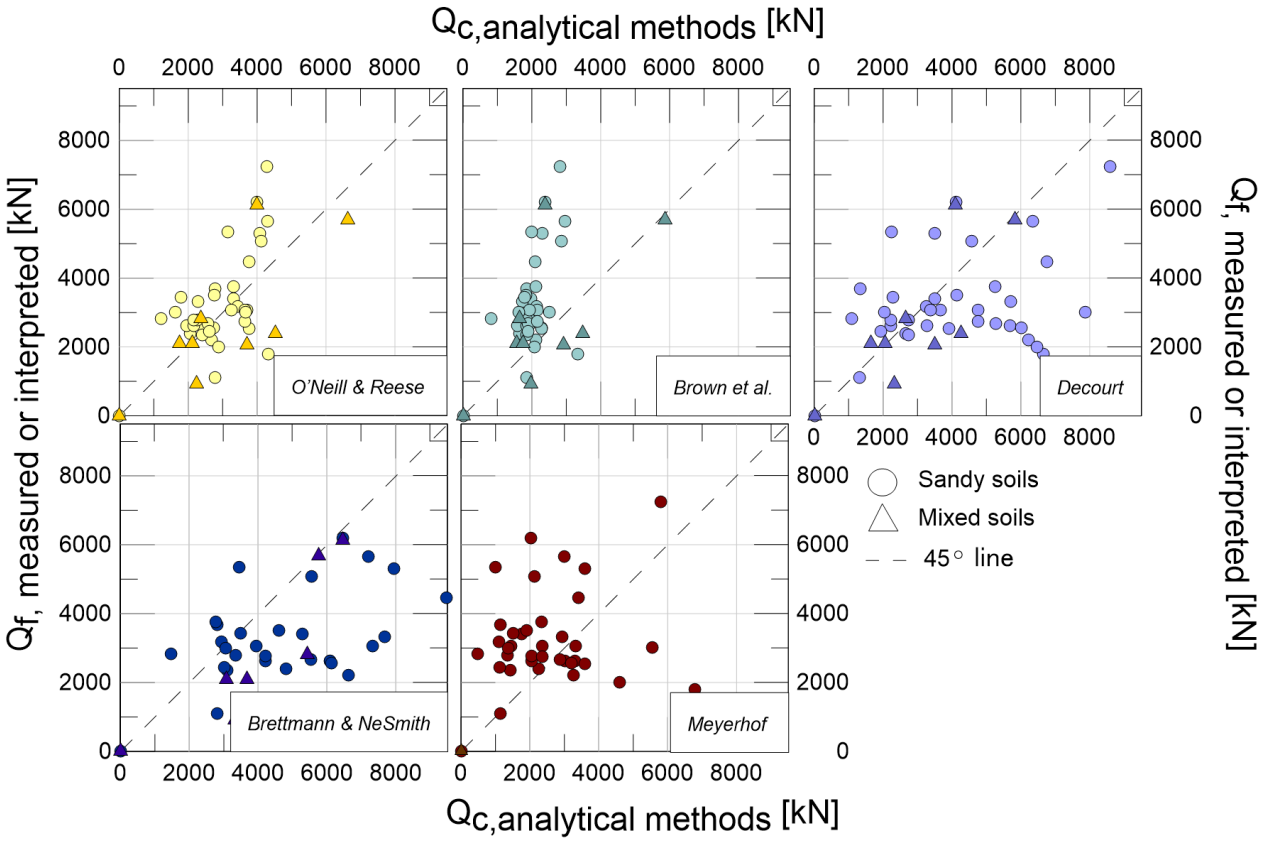

Figure 15. Interpreted failure load versus the axial load capacity estimated analytically from the SPT methods

Q_f/Q_c ratio in Figure 16. It can be observed that regardless of the pile slenderness, a general trend of capacity underestimation using CPT-based methods is observed for all pile geometries, ranging from small to large slenderness ratios (i.e., more data plot above the 1.0 line).

Figure 17 compares the axial load at failure (measured or interpreted) with the axial capacity predicted by the different analytical methods by separating the methods based on their empirical derivation: the upper row corresponds to the methods developed specifically for drilled displacement piles (i.e., Brettmann and NeSmith (2000; 2005) for SPT and CPT data, and Bustamante and Gianeselli (1993; 1998)). The second row depicts all remaining methods. Similary, the three columns categorize the results into sandy soils (left column), clayey soils (center), and the mixed soils (right column). Unfortunately, the desired improved accuracy (when using methods developed for DDPs specifically) is not recognizable in Figure 17. The DDP methods and the "other" methods shows similar data scatter.

According to Siegel *et al*. (2007), the installation of drilled displacement piles in sandy soils results in densification of the soil surrounding the pile and an increase in lateral stresses. In this study, an increase in CPT tip resistance (q_t) was encountered following several pile installations. Even though data were limited, the available average CPT tip resistance (q_t) and the SPT-based N60 resistance measured before the pile installation was compared with the Q_f/Q_c ratio for each sandy and mixed soil site. The average tip resistance (q_t) was computed as the arithmetic mean of the q_t values at different depths for sandy and clayey soils. For mixed types of soils, the average tip resistance was computed for soils with a soil index behavior (I_c) higher and lower than 2.6, clay-like and sand-like behavior, respectively; with those two values, and the percentage of each type of soil within the soil profile, a weighted average was calculated. Figure 18 shows the Q_f/Q_c ratio against the average pre-pile installation cone tip resistance (q_t) (top row) and the SPT N60 values (bottom row) for sandy (a), clayey (b) and mixed soils (c). For soils with initially low strength (e.g., q_t = 5-10 kPa, or N60<15) Figure 18 suggests an inverse relationship between the soil resistance, (i.e., qt or N60). The ratio between failure load and the estimated capacity seems to follow a slight downward trend. Even though the soil improvement during pile construction is a complex topic with high variability, different authors have proven that the higher the initial soil resistance (i.e., high initial soil strength), the less improvement the soil experiences due to DDP installation. Consequently, a higher accuracy, and a Q_f/Q_c ratio closer to one is obtained for dense sands and stiffer silt mixtures since the soil does not experience great changes. On the other hand, for looser soils, the implementation of the analytical methods without soil improvement considerations can lead to the underestimation (or conservatism) of the pile's capacity Q_f/Q_c >1. For clayey soils no relationship between the ratio Q_f/Q_c and q_t

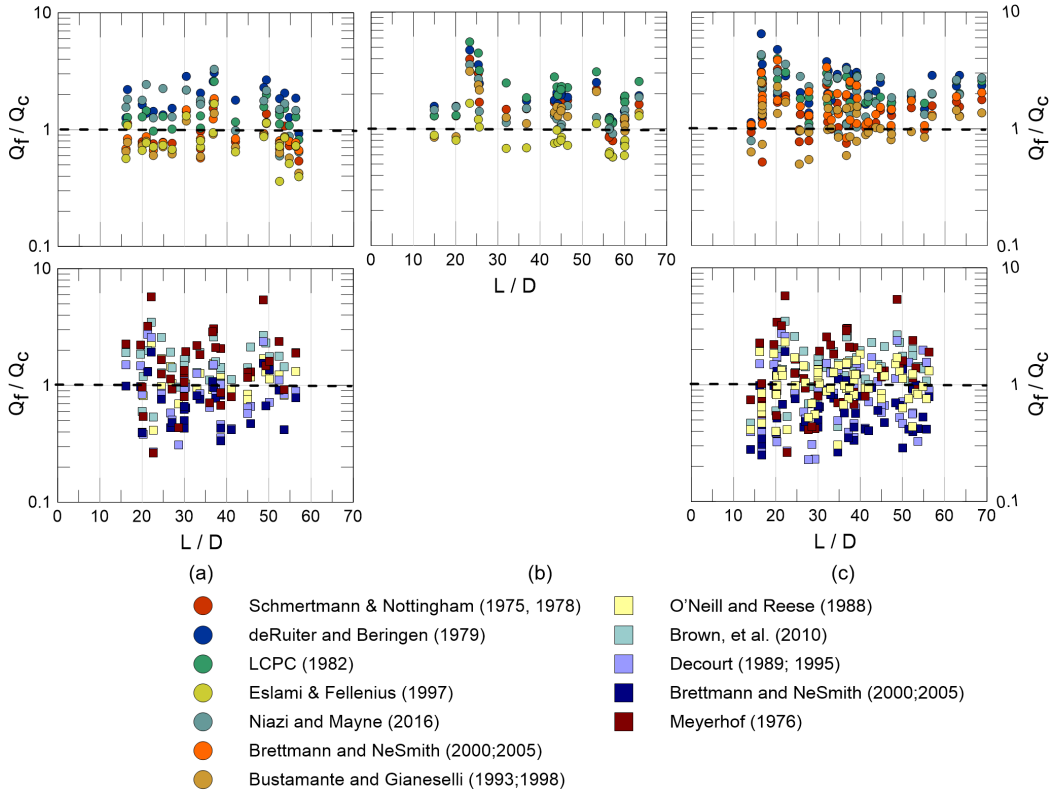

Figure 16. L/D ratio versus the Q_f/Q_c ratio. Columns: (a) Mostly sandy soils. (b) Mostly clay soils, (c) Mixed soils

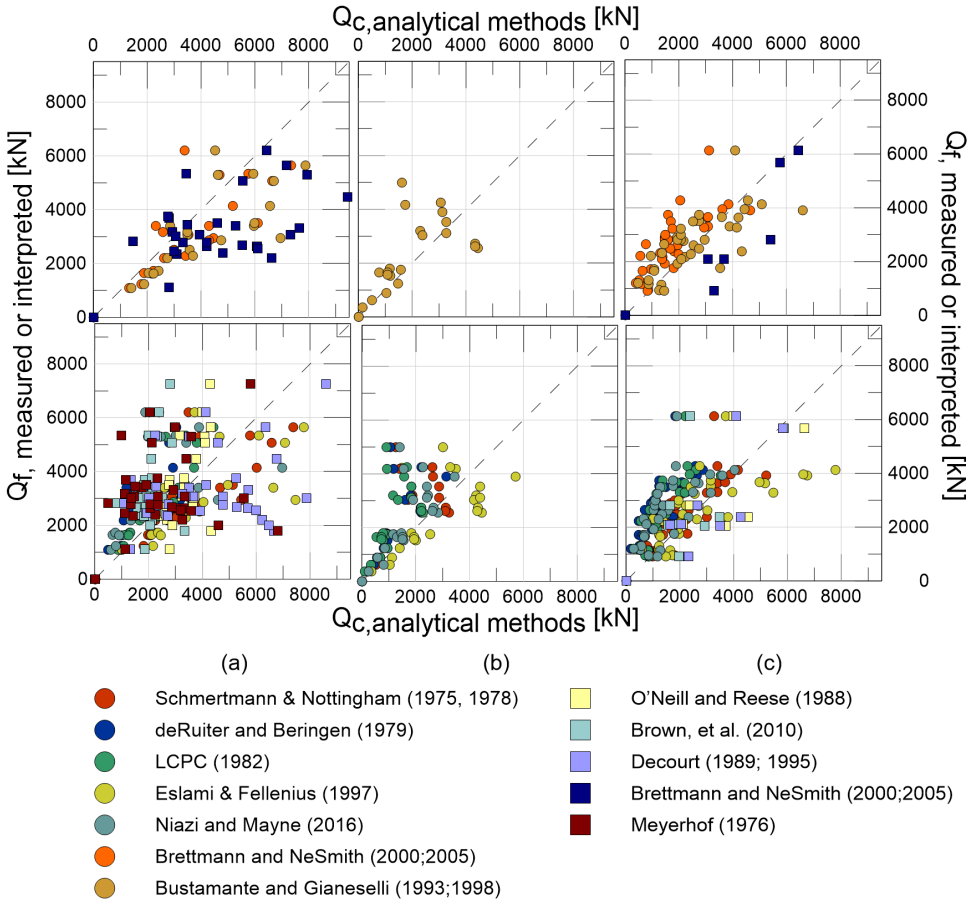

Figure 17. Measured or interpreted failure load versus the axial load capacity estimated analytically, comparison according to the installation method for which the analytical methods were developed. Columns: (a) Mostly sandy soils. (b) Mostly clay soils, (c) Mixed soils

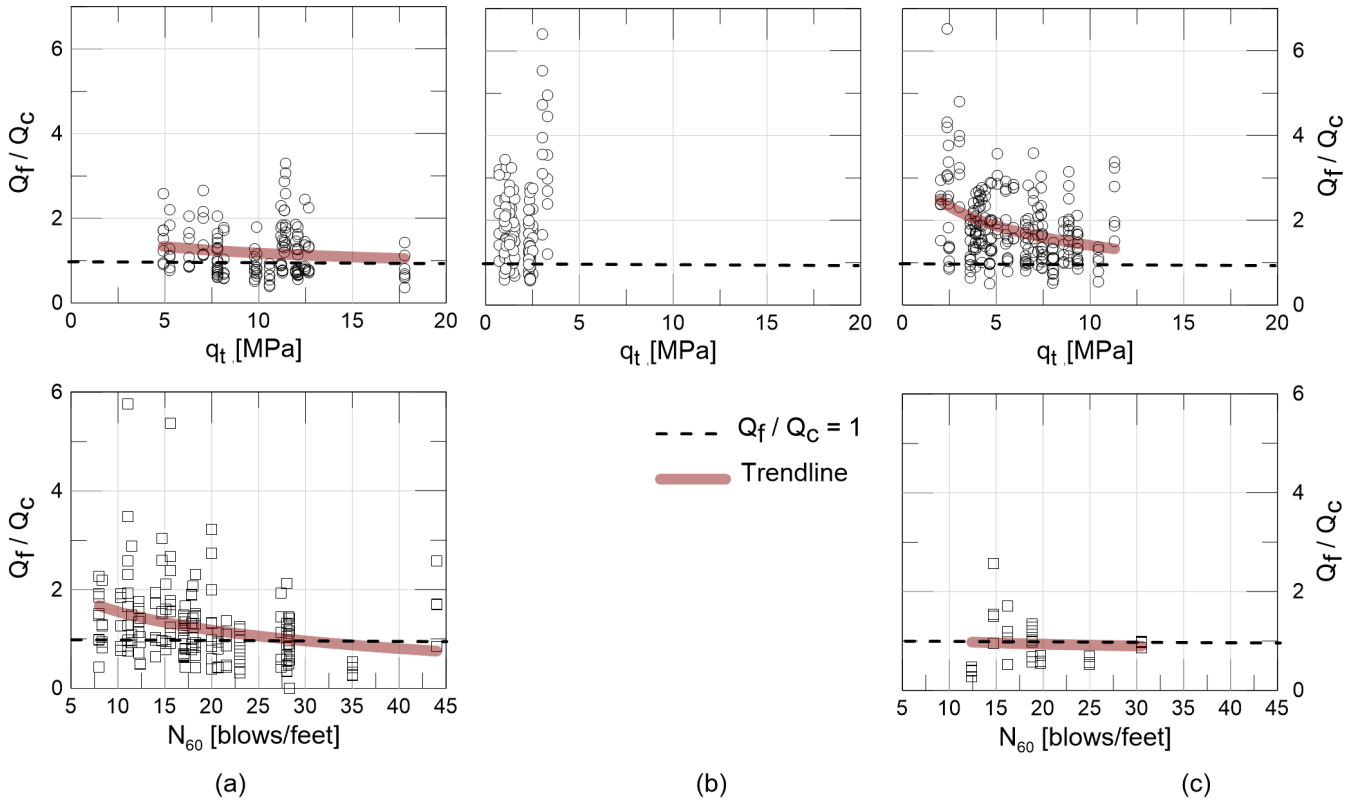

Figure 18. Average cone tip resistance (q_t) in MPa, and N_{60} versus the Q_f/Q_c ratio. (a) Mostly sandy soils, (b) Clay soils, and (c) Mixed soils

was found, this is due to the unique degree of "improvement" or "relaxation" this type of soil can experience.

Summary and Conclusions

Current practice for the design of deep foundations employs different empirical methods developed between 1975 and today. While many of the methods have been validated and calibrated to approximate the actual failure load of driven and bored piles, only few methods account for the installation and performance effects of drilled displacement piles (DDPs). A database of 55 construction sites, in which more than 120 DDP were installed and tested, was utilized to evaluate the predictive accuracy of CPT and SPT based direct methods in estimating axial pile load capacity for DDPs in sand like, clay like, and mixed soil sites.

Prior to comparing predicted and measured axial capacities of drilled displacement piles, this study first investigated a variety of literature-based methods to interpret/estimate pile failure in the absence of experimentally reached failure. A comparison of eleven different methods, including the "Load at 10% of the pile diameter" method suggested that Van der Veen's Criteria (1953) provided the best match between estimated and measured failure. This method was closely followed by Butler & Hoy (1977), which slightly underpredicted the in-situ failure and L1-L2 method by Hirany and Kulhawy (1989) which slightly overpredicted the in-situ failure load of the 100+ piles investigated. The Decourt Method and Chin-Kondner Extrapolation methods overestimate the DDP failure loads across a large spectrum, while the De Beer's Criterion (1968) and the DOL Method generally underestimate the failure load of the drilled displacement piles. A modification factor to Davisson's method for DDP interpretation was iterated following suggestions from Perlow (2020). With a modification factor of 4 to the last term of Davisson's failure interpretation equation, the failure load of DDPs can be much more accurately estimated and extrapolated from its original application to driven piles.

When comparing in-situ failure to analytically predicted failure, almost all examined methods underpredict the capacity of the piles. Among all CPT-based methods, Brettmann and NeSmith (2000; 2005) showed a better agreement between the measured and analytically failure load for sandy soils, the Bustamante and Gianeselli (1993;1998) method showed the most favorable approximation of the pile failure loads for mixed type of soils, and Eslami and Fellenius (1997) provided a more accurate estimation for clayey soils. The performance of the SPT direct methods was also evaluated, the most acceptable Q_f and Q_c agreement was achieved with the O'Neill and Reese (1988) method for sandy and mixed type of soils. However, overall, the authors recommend against the use of SPT-based prediction given the large scatter in analytically determined axial pile capacities and the uncertainty associated with estimating shear strength from SPT data needed for the SPT-based predictions.

The maximum axial load achieved during the pile tests was 200% to 300% of the design load; at this level of force, the settlement of the piles was considerably far from the plunging behavior. The higher pile capacity could be partially attributed to the higher resistance achieved due to the instal-

lation effects. Favorable ground improvement effects such as the densification of soil surrounding the DDP can translate favorably into more accurate predictions of the actual pile failure load and represent an added factor of safety during the design phase, as pile design often relies on pre-pile installation based in-situ data.

In summary, the estimation of pile capacity and pile failure remains a function of high quality in-situ data and methods specifically developed for a certain pile type, inherently accounting for pile installation and construction effects. The current data reduces (but does not eliminate this gap) by providing recommendations for more accurately estimating pile failure from load test data and predicting pile capacities using existing methods.

Acknowledgments

This work was supported in part by the DFI Technical Committee Project Fund as well as by the National Science Foundation Grant CMMI 1752303. We thank the following professionals for their unreserved support and their willingness to share data generously and continuously: Sam Warren (Farrell Design-Build, Inc.), Piyush Sharma and Danny Cohen (Morris- Shea Bridge Co., Inc.), Morgan NeSmith (Berkel and Company), Peter Faust (Malcolm Drilling), Tim Siegel (DBA), Derek Deutscher (formerly Condon Johnson), and Franz-Werner Gerressen (Bauer Maschinen). Furthermore, the authors are grateful for all intellectual exchange and discussion during this study, specifically with: Morgan NeSmith (Berkel) as well as the committee members of the ACIP and DD committee under the leadership of Jonathan Huff (Goettle).

References

AASHTO (American Association of State Highway and Transportation Officials) (2008). *Load and* Resistance *Factor Design Bridge Design Specifications*. Washington, D.C.:

ASTM (American Society for Testing and Materials) (2020). *Standard Test Methods for Deep Foundation Elements* Under *Static Axial Compressive Load*. ASTM International, Standard D1143M. West Conshohocken, PA. doi: 10.1520/D1143_D1143M-20.

Baligh, F. A., & Abdelrahman G. E. (2005-2006). Modification of Davisson's method. Proceedings of the 16th International Conference on Soil Mechanics and Geotechnical Engineering. *International Society for Soil Mechanics and Geotechnical Engineering, 2079-2082*. doi:10.3233/978-1-61499-656-9-2079

Basu, P., & Prezzi M. (2009). Design and Applications of Drilled Displacement (Screw) Piles. Publication FHWA/IN/JTRP-2009/28. *Joint Transportation Research Program, Indiana Department of Transportation and Purdue University.* doi.org/10.5703/1288284314278

Brettmann, T., & NeSmith W. (2005). *Advances in auger pressure grouted piles: design, construction, and testing*. Advances in Designing and Testing Deep Foundations. Austin, Texas, United States, ASCE, 262–274. doi:10.1061/40772(170)5

Brown, D.A., Turner, J.P., & Castelli, R.J. (2010). *Drilled shafts: construction procedures and LRFD design methods*. National Highway Institute, U.S. Department of Transportation, Federal Highway Administration. Publication No. FHWA-NHI-10-016, Washington, D.C.

Bustamante, M., & Gianeselli, L. (1982*)*. Pile bearing capacity predictions by means of static penetrometer CPT. *Proc*., *2nd European Symposium on Penetration Testing (ESOPT-II)*, 2, 493–500.

Bustamante, M., & Gianeselli., L. (1993). Design of auger displacement piles from in-situ tests. *Deep Foundations on Bored and Auger Piles*, BAP II, Balkema: Rotterdam, 21–34.

Bustamante, M., & Gianeselli., L. (1998). Installation parameters and capacity of screwed piles. *Deep Foundations on Bored and Auger Piles*, BAP III, Balkema: Rotterdam, 95–108.

Butler, H.D. & Hoy, H.E. (1977). *User's manual for the Texas quick load method for foundation load testing.* Department of Transportation Federal Highway Administration Office of Development. Publication No. *FHWA*-IP-77-8, Washington, D.C.

Caltrans (California Department of Transportation) (2015). *Foundation Manual Chapter 8, Static Pile Load Testing and Pile dynamic Analysis.* Revision No. 2, California. Retrieved from https://dot.ca.gov.

Chin, F.K. (1970). Estimation of the Ultimate Load of Piles Not Carried to Failure. *Proceedings of Second Southeast Asian Conference on Soil Engineering*, 81-92.

Davisson, M. T. (1972). High-capacity piles. *Proceedings of Lecture Series on Innovations in Foundation Construction,* American Society of Civil Engineers (ASCE), Illinois Section, Chicago, 81 - 112.

DeBeer, E. E. (1968). Proefondervindlijke bijdrage tot de studie van het grensdraag vermogen van zand onder funderingen op staal. (Experimental contribution to the study of the limit bearing capacity of sand under *foundations* on steel). *Tijdshift der oOpenbar Verken van Belgie,* No. 6.

De Ruiter, J., & Beringen, F. L. (1979). Pile foundations for large North Sea structures. *Marine Georesources & Geotechnology*, 3, 267–314.

Decourt, L. (1995). Prediction of load-settlement relationships for foundations on the basis of the SPT. Ciclo de Conferencias Internationale, Leonardo Zeevaert, UNAM, Mexico, 85-104.

Decourt, L. (1999). Behavior of foundations under working load conditions. Proceedings of the 11th Pan-American Conference on Soil Mechanics and Geotechnical Engineering, Brazil, 4, 453 - 488.

Dotson D. W. (2013). Direct solution of the Brinch-Hansen 90% Pile Ultimate Failure Load. Deep Foundation Institute (DFI)- Journal of Deep Foundation Institute, 7(1), 18-21.

Eslami, A., & Fellenius, B.H. (1995). Toe bearing capacity of piles from cone penetration test (CPT) data. Procedure of the International Symposium on Cone Penetration Testing. Linköping, Sweden, Swedish Geotechnical Institute, SGI, 2.

Eslami, A., & Fellenius, B. H. (1997). Pile capacity by direct CPT and CPTU methods applied to 102 case histories. Canadian Geotechnical Journal, 34, 886–904.

Fellenius B. H. (2001). What capacity value to choose from the results of a static loading test. We have determined the capacity, then what?. Deep Foundation Institute, Fulcrum, Winter, 19 – 22 and Fall 2001, 23 - 26.

FHWA (Federal Highway Administration) (1992). Static Testing of Deep Foundations. U.S. Department of Transportation. Washington, D.C. 20590. Publication No. FHWA-SA-91-042, Washington, D.C.

Hansen, J.B., (1963). Discussion on hyperbolic stress-strain response. Cohesive soils. *American Society of Civil Engineers, ASCE, Journal for Soil Mechanics and Foundation Engineering*, 89, 241 - 242.

Hara, A., Ohta, T., Niwa, M., Tanaka, S., & Banno, T. (1974). Shear modulus and shear strength of cohesive soils. *Soils and Foundations*, 14, 1-12. doi.org/10.3208/sandf1972.14.3_1

Hansen, J.B. (1961). A general formula for bearing capacity. *Ingeniøren International Edition*, Copenhagen, 5, 38-46.

Hogg, R. V., & Craig, A. T. (1995). *Introduction to mathematical statistics*. Ed. 5. Upper Saddle River, New Jersey, Prentice Hall.

IBC (International Building Code) (2018*). Chapter 8 - Soils and Foundations.* International Code Council.

Meyerhof, G. G. (1976). Bearing Capacity and Settlement of Pile Foundations. *Journal of the Geotechnical* Engineering *Division*, 102(3), 195–228. doi: 10.1061/AJGEB6.0000243

Moshfeghi, S., & Eslami, A. (2018). Failure analysis of CPT-based direct methods for axial capacity of driven piles in sand. *Georisk: Assessment and Management of Risk for Engineered Systems and Geohazards.* 13, 1-19.

Nesmith, W.M. (2002). Static capacity analysis of augered, pressure-injected displacement piles. *Proceedings, International Deep Foundations Congress, M. O'Neill and F. Townsend.* Publication No.116, 1174-1186.

NeSmith W. M. & Siegel, T. C. (2009). Shortcomings of the Davisson Offset Limit applied to axial load *compressive* load test on cast-in-place piles. *American Society of Civil Engineers. International Foundation Congress and Equipment Expo*. doi:10.1061/41021(335)71

Niazi, F., and Mayne, P., 2016. CPTu-based enhanced UniCone method for pile capacity. Engineering Geology. 212. 10.1016/j.enggeo.2016.07.010.

O'Neill, M. W., & Reese, L. C. (1988). Drilled Shafts: Construction Procedures and Design Methods. *ADSC (The International Association of Foundation Drilling)*. Publication No. ADSC-TL4, 471

Peck, R. B., Hanson, W. E., & Thornburn, T. H. (2nd Edition) (1974). *Foundation engineering*. New York: Wiley.

Perlow M. (2020). A soil quake Davisson Offset Method for Drilled Foundations. *Deep Foundation Institute 45th Annual Conference*, USA, Red Hook, NY, 183

Prezzi, M. & Basu D. (2010). Drilled displacement piles–current practice and design. *Journal of the Deep Foundations Institute,* 4(1), 3–20.

Robertson, P. K., Cabal K. L., 2015. Guide to Cone Penetration Testing for Geotechnical Engineering. Gregg Drilling & Testing, Inc.

Schmertmann, J. H. (1978). Guidelines for Cone Penetration Test, Performance and Design. *Rep. No. FHWA-TS-78-209, U.S. Department of Transportation*, Washington, D.C., 145.

Shah, F.R. & Deng, L. (2016). Comparing Axial Behavior of Non-Displacement and Displacement Piles using Field Load Tests. *69th CGS Conference Vancouver*, B.C. Canada.

Siegel, T. C., NeSmith W. M., & Cargill, P. E. (2007). Ground Improvement resulting from Installation of Drilled Displacement Piles. *Deep Foundation Institute 32nd Annual Conference*, Colorado Springs.

Siegel, T.C., Day, T.J., Turner, B., and Faust, P. (2019). Measured end resistance of CFA and drilled displacement piles in San Francisco Area alluvial clay. DFI Journal - The Journal of the Deep Foundations Institute, 12 (3), 186-189

Stacho, Jakub & Ladicsova, E. (2014). Numerical analysis of drilled displacement system piles. International Multidisciplinary Scientific GeoConference Surveying Geology and Mining Ecology Management, SGEM. 2. 665-671

Stuedlein, A. W., Reddy, S. C., & Evans, T. M. (2014). Interpretation of augered cast in place using static load tests. *Deep Foundation Institute- Journal of Deep Foundation Institute*, 8(1), 39-47.

Van der Veen, C. (1953). The bearing capacity of a pile proceedings. *3rd International Conference on Soil Mechanics and Foundation Engineering*, 2, 84-90.

DFI Journal Underwriters